Front. Mech. Eng. 2024, 19(1): 6
https://doi.org/10.1007/s11465-023-0772-0

REVIEW ARTICLE

Review on piezoelectric actuators: materials, classifications, applications, and recent trends

Xuyang ZHOU[a], Shuang WU[b], Xiaoxu WANG[b], Zhenshan WANG[a], Qixuan ZHU[a], Jinshuai SUN[a], Panfeng HUANG[b], Xuewen WANG[a], Wei HUANG[a], Qianbo LU (✉)[a,c]

[a] *Institute of Flexible Electronics (IFE), Northwestern Polytechnical University, Xi'an 710072, China*
[b] *School of Automation, Northwestern Polytechnical University, Xi'an 710072, China*
[c] *Key Laboratory of Flexible Electronics of Zhejiang Province, Ningbo Institute of Northwestern Polytechnical University, Ningbo 315103, China*
✉ *Corresponding author. E-mail: iamqlu@nwpu.edu.cn (Qianbo LU)*

ABSTRACT Piezoelectric actuators are a class of actuators that precisely transfer input electric energy into displacement, force, or movement outputs efficiently via inverse piezoelectric effect-based electromechanical coupling. Various types of piezoelectric actuators have sprung up and gained widespread use in various applications in terms of compelling attributes, such as high precision, flexibility of stoke, immunity to electromagnetic interference, and structural scalability. This paper systematically reviews the piezoelectric materials, operating principles, representative schemes, characteristics, and potential applications of each mainstream type of piezoelectric actuator. Herein, we intend to provide a more scientific and nuanced perspective to classify piezoelectric actuators into direct and indirect categories with several subcategories. In addition, this review outlines the pros and cons and the future development trends for all kinds of piezoelectric actuators by exploring the relations and mechanisms behind them. The rich content and detailed comparison can help build an in-depth and holistic understanding of piezoelectric actuators and pave the way for future research and the selection of practical applications.

KEYWORDS piezoelectric actuator, piezoelectric effect, amplified piezoelectric actuator, ultrasonic actuator, stepping actuator, piezoelectric polymer

1 Introduction

Recent advances in science and engineering have led to a rapid expansion of applications of ultraprecision positioning and driving technologies. As listed in Table 1, piezoelectric actuators demonstrate superiority in nanometer-scale resolution, fast response, and immunity to magnetic interference, outperforming their counterparts, such as shape-memory alloy actuators and magnetostrictive actuators [1–3], in applications of precision manufacturing, displacement output, medical treatment, and microfluidics control (Fig. 1). Additionally, the structural scalability and excellent load capacity make piezoelectric actuators a promising candidate in the fields of robotics, automation, industrial inspection [4], aerospace, and defense. While exhibiting plenty of advantages, piezoelectric actuators suffer from limitations, such as short stroke at the early stage and strong nonlinearity, in terms of the fundamental principle of inverse piezoelectric effect [5,6]. Highly nonlinear behavior, such as hysteresis and creep, leads to degraded motion accuracy and repeatability, the former usually accounting for approximately 10%–15% of tracking error [7].

The development of various types of piezoelectric actuators has been a subject of continuing interest over the past decades, and researchers have explored numerous approaches to achieve large strokes and other improved performance [8,9]. For example, piezoelectric materials are iteratively updated, thus injecting vitality into the community with new types of materials. Some researchers have tried to modify the working principle and structural design, which have evolved into different types of piezoelectric actuators, such as ultrasonic- and inchworm-based actuators. Several reviews [8,9] focused on the summarization of the recent progress of piezoelectric actuators, whereas most conventional articles classified piezoelectric actuators from a performance or structure point of view. The lack of a scientific

Received June 4, 2023; accepted October 8, 2023

Table 1 Comparison of different types of actuators and their principles, accuracy, advantages, and disadvantages

Actuator type	Driving principle	Accuracy	Advantages	Disadvantages
Electrostatic	Coulomb force	Below the micron	High efficiency, small size, insensitive to the outside temperature	Small output force, harsh environment requirements
Electromagnetic	Electromagnetic induction	Micron	High response frequency, reliable operation, low cost, better output, insensitive to the outside temperature	Large volume, serious heat, loud noise
Shape-memory alloys	Shape-memory effect	Micron	Better flexibility, small size, large deformation, high energy density	Sensitive to external temperature, slow response, low efficiency
Magnetostrictive	Magnetostrictive effect	Below the micron	Large driving force, no fatigue and heat loss	Sensitive to electromagnetic magnetic fields, hysteresis
Electrostrictive	Electrostrictive effect	Below the nanoscale	Low creep, better reproducibility	Sensitive to temperature, average energy density
Photostrictive	Photostrictive effect	Micron	Antielectromagnetic interference, lightweight, miniaturization, high response frequency	Sensitive to temperature, low efficiency
Piezoelectric	Inverse piezoelectric effect	Subnanometer	Antimagnetic interference, high efficiency, high response frequency	Hysteresis, creep, more sensitive to temperature

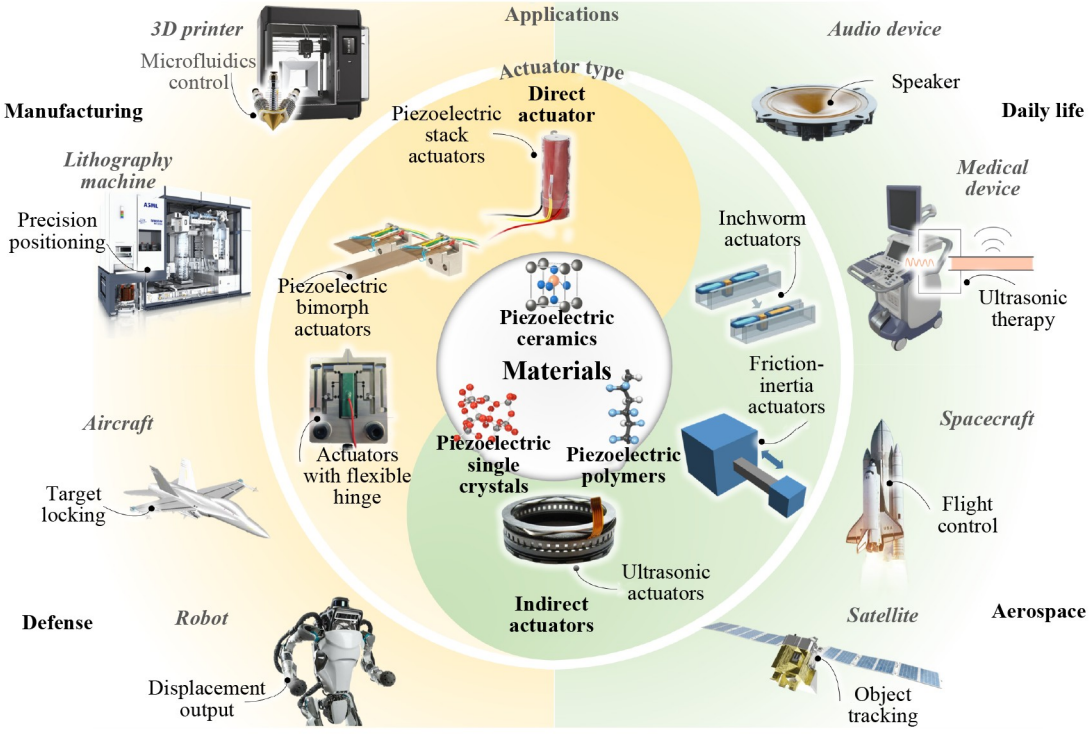

Fig. 1 Piezoelectric actuators and their fields of application.

perspective led to classification ambiguity or an insufficient grasp of some future development trends. A systematic review of the piezoelectric actuators, including the materials, operating principles, representative schemes, and development trends, has remained elusive. Herein, we divide piezoelectric actuators into direct and indirect categories with several subcategories from a more nuanced perspective, which helps cover mainstream and cutting-edge piezoelectric actuators and provides a more in-depth insight into concern in the engineering field.

Direct piezoelectric actuators refer to piezoelectric actuators that directly use the stretching effect of the piezoelectric film without complicated structural and principal design. Therefore, it incorporates features, such as high precision, simple construction, and rapid response [8,10], and is especially suitable for short-stroke applications with high precision requirements. This big class is further divided into unimorph, bimorph, and actuators with amplified schemes according to the operation principle. From a structural point of view, the unimorph and bimorph ones are the simple variants of a monolithic film-based actuator, which is the basis of the direct piezoelectric actuators, while amplified schemes use the stacking strategy [11,12], and flexible hinges are advanced variants to address the short stroke and low load capacity issues straightforwardly by amplification. Notably, unimorph, bimorph, and stacks can be used in conjunction with flexible hinges to combine the merits together [13,14], improving other performance [15,16].

In contrast to direct piezoelectric actuators, indirect piezoelectric actuators convert the deformation of piezoelectric materials into indirect displacement via some complicated structures, and the relation between the deformation of the materials and the output displacement is more than simple amplification. By using strategies, such as repeating and stepping, indirect piezoelectric actuators can achieve a larger stroke and responses with more degrees of freedom (DOFs) [10,17,18], while the potential cost is the increased complexity and the decreased resolution. Depending on the working principle, this big class is further divided into two subcategories, ultrasonic actuators [19], and stepping actuators [8]. They both have subclasses, which will be introduced in detail.

Figure 2 presents a comprehensive classification framework, and it constitutes the main body of this review together with the necessary introduction of the piezoelectric effect principle and piezoelectric materials. Accordingly, this paper is organized as follows: Section 2 briefly outlines the piezoelectric effect principle and the piezoelectric materials; Section 3 elaborates on direct piezoelectric actuators, including unimorph, bimorph, and amplified piezoelectric actuators; Section 4 divides indirect piezoelectric actuators into ultrasonic motors and stepping actuators and introduces them one by one; Section 5 compares the pros and cons of different types of actuators, refining the characteristics of types of piezoelectric actuators from a scientific point of view; and Section 6 presents the conclusions and outlook on future developments.

2 Piezoelectric effect and piezoelectric materials

2.1 Background

The piezoelectric effect denotes the ability of certain materials to generate an electric charge in response to applied mechanical stress, whereas the inverse effect is the reverse, as shown in Fig. 3. Generally, the piezoelectric effect stems from the electromechanical coupling between the dielectric and elastic properties. Dielectric properties mainly refer to the relationship between electrical displacement and electric field, and elastic properties refer to the relationship between stress and strain. The IEEE standard on piezoelectricity [20] has been established for decades based on fundamental contributions from Voigt [21], Cady [22], Heising [23], Mason [24], Mindlin [25], Tiersten et al. [26,27], etc.

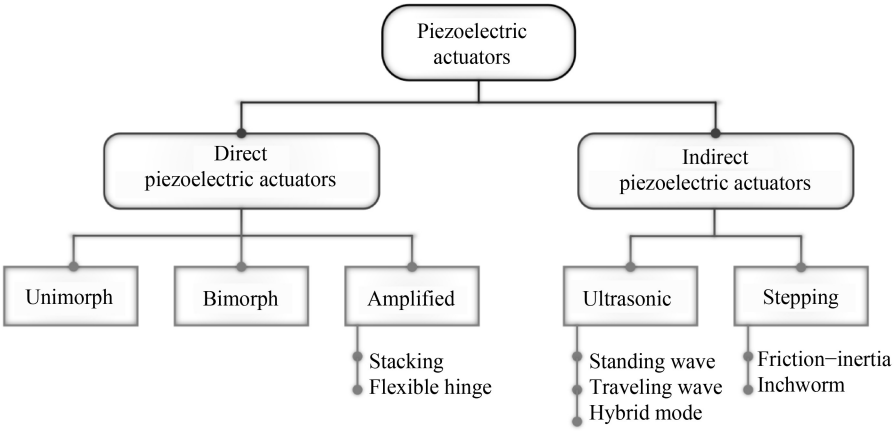

Fig. 2 Classification diagram of piezoelectric actuators.

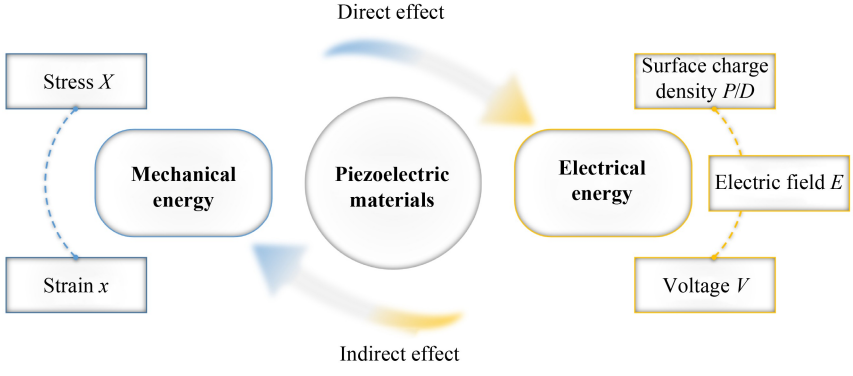

Fig. 3 Piezoelectric effect energy conversion relationship.

Figure 4 shows the schematic of the basic working modes of direct and indirect piezoelectric effects, including the longitudinal, transversal, and shear modes. The piezoelectric coupling coefficients used in each case are listed in Table 2.

Piezoelectric constitutive equations are the underpinning for the design and analysis of piezoelectric actuators, which can be obtained by experimental results and rigorous derivation from thermodynamic theory [28]. In consideration of different boundary conditions, mechanical and electrical boundary conditions can be combined in pairs; therefore, four sets of piezoelectric constitutive equations can describe the piezoelectric effect. In the different equations, the selection of independent and dependent variables is also diverse. Usually, different boundary conditions are used as independent variables. These formulas reflect the relationship between the mechanics and electricity of the piezoelectric material, and the essence behind them is the same and can be converted into each other [20]. These constitutive equations clearly elaborate the principle and relation of the piezoelectric effect and play a crucial role in practical analysis and simulation, such as finite element analysis. In practical applications, the piezoelectric equations of the first and second types are commonly used because the electrical displacement D_i (in the third and fourth types), as an artificially defined quantity, cannot be effectively controlled.

The existence of nonlinear behavior in piezoelectric actuators leads to the degradation of positioning accuracy. This behavior mainly includes hysteresis and creep effects. Hysteresis refers to a nonlinear phenomenon exhibiting a loop and branched relationship between the applied voltage and output displacement. It depends upon the current input voltage, history of input, and input signal frequency [29]. This behavior is positively related to frequency [7]. Creep behavior refers to slight variations in displacement after input signal change. It becomes less dominant at high frequencies [30]. The control of piezoelectric actuators is critical due to the above behavior, which must be appropriately handled in practical engineering applications [31]. When facing the nonlinear factors of the actuator itself and the external disturbances, in contrast to the traditional proportional integral derivative (PID) control strategy, the trend in recent years is to adopt sliding mode control—a kind of robust control method to cope with them [32], which even includes the scheme of introducing neural network [33] and reinforcement learning algorithm [34].

2.2 Piezoelectric materials

Materials that can exhibit the piezoelectric effect are called piezoelectric materials [35]. Specifically, a piezoelectric material is a special type of dielectric material in terms of its noncentrosymmetric crystal structure [36].

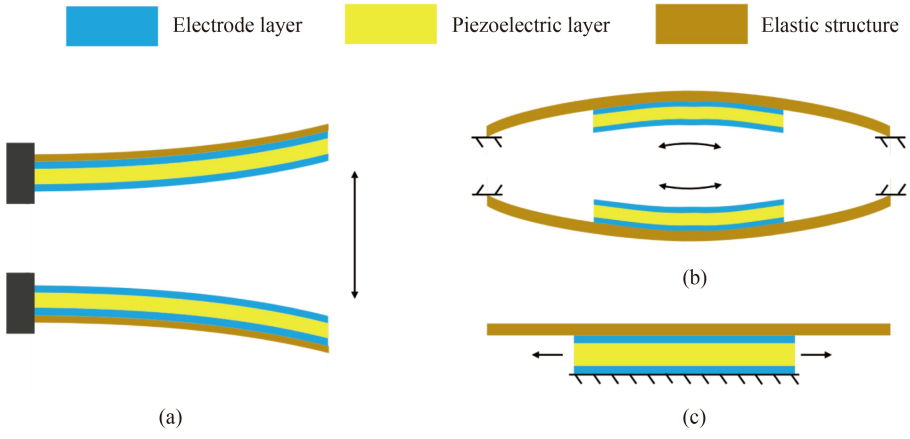

Fig. 4 Unimorph piezoelectric actuator: (a) bending mode 1, (b) bending mode 2, and (c) linear expansion/retraction mode.

Table 2 Coupling coefficients for different modes

Type	Mode	Orientation of stress	Orientation of charge	Coupling coefficient
Direct piezoelectric effect	Longitudinal	3	3	d_{33}
	Transversal	3	1	d_{31}
	Shear	1	5	d_{15}
Indirect piezoelectric effect	Longitudinal	3	3	e_{33}
	Transversal	3	1	e_{31}
	Shear	1	5	e_{15}

Piezoelectric materials can be classified into single crystals, piezoelectric ceramics, and polymers. Table 3 summarizes the properties of various piezoelectric materials. Single crystals can achieve a more extensive range of the piezoelectric constant via different doping methods and thus, the highest coefficient, while better specifications usually result in higher cost and greater fragility. Most common commercial piezoelectric materials, piezoelectric ceramics, usually have a higher piezoelectric constant and dielectric constant, which result in a stronger piezoelectric effect. Polymers exhibit low piezoelectricity in terms of the relatively small piezoelectric constant and dielectric constant while they show better flexibility, low density, low acoustic impedance, and easy processing. A brief introduction to these types is given below.

Piezoelectric single crystals contain natural and synthetic ones. The former representatives are quartz and Rochelle salt [37–39], and the latter representatives are PMN-PT, PIN-PT, PZN-PT, etc. [40]. The piezoelectricity of natural single-crystal piezoelectric materials originates from their natural structural growth, whereas that of relaxor ferroelectrics represented by PMN-PT comes from artificial control [41]. The latter gained widespread attention in the mid-1990s with the gradual maturity of the relaxor ferroelectric single-crystal growth technology and obtained astonishing piezoelectric coefficients in related experiments. Park and Shrout [42] reported amazing PMN-PT and PZN-PT, whose piezoelectric coefficient d_{33} and electromechanical coupling k_{33} can reach up to 2500 pC/N and a level of > 90%, respectively. In recent years, Li et al. [43] have also realized an Sm-doped PMN-PT single crystal with a coupling coefficient d_{33} up to 3400–4100 pC/N. However, the excellent coupling coefficients result in high cost and process complexity [44].

$BaTiO_3$ [45,46], AlN [47], and piezoelectric lead zirconate titanate (PZT) [48] are representative materials among the group of piezoelectric ceramics. The piezoelectric effect is described as the change in ion equilibrium and the creation of a nonzero crystal dipole moment through the ions' motion under stress. Among them, PZT ceramics, discovered in the 1950s [5], with morphotropic phase boundary [49,50] compositions have prominent figures of merit, such as an electromechanical coupling factor $k_{33} > 0.60$, a piezoelectric coefficient $d_{33} > 200$ pC/N, low cost of manufacture, and a relatively high Curie temperature T_c (~350 °C). These characteristics make it widely used in many fields. However, in consideration of the ever-increasing medical diagnostics and precision manufacturing demands, piezoelectric ceramics that have excellent piezoelectricity (high piezoelectricity with high-temperature stability and broad usage temperature ranges) are required. Work in this area must resolve the dilemma in which piezoelectricity and Curie temperature can only be enhanced at the expense of each other; a breakthrough was achieved recently [51] by using a seed-passivated texturing process to fabricate textured PZT ceramics.

Piezoelectric polymers [52] are a class of piezoelectric materials with a relatively few applications. They can be further classified as bulk polymers, piezoelectric composite polymers, and voided charged polymers [53,54]. Typical bulk polymers are polyvinylidene fluoride (PVDF) [55,56], polyamides, Parylene-C [57], polyimide [58,59], and polyvinylidene chloride [54]. These polymers are mostly organic materials. Piezoelectric composites are polymers with a mixture of inorganic piezoelectric materials [60,61], which combine the advantages of two different materials [62]. Voided charged polymers, also known as porous/cellular polymers, have internal gas voids, which can exhibit piezoelectric effects when the polymer surface around the gas voids is electrically charged [63]. The filler gases can be N_2, CO_2, etc., which correspond to different properties [64,65]. The gas choice and the charge method of the voids are two main ways to

Table 3 Piezoelectric coupling coefficients of different piezoelectric inorganic and organic materials

Compound	Material	Type	Piezoelectric constants		Ref.
			d_{33}/(pC·N^{-1})	d_{31}/(pC·N^{-1})	
Inorganic	α-Quartz	Single crystal	2.31	–	[37]
	$LiNbO_3$		6	−1	[37]
	PMN-PT		2500	–	[42]
	PZN-PT		2455	−1204	[40]
	PIN-PT		1600	–	[41]
	AlN	Ceramic	5.5	−2.0	[47]
	$BaTiO_3$		191	−79	[35]
	PZT-5A		374	−171	[48]
	PZT-5H		650	−320	[35]
Organic	PVDF	Polymer	25	–	[56]
	Polyimide		2.5–16.5	–	[53]

tune the piezoelectric effect [66]. This material is more important in some special fields, such as medical treatment and flexible electronics, than in others.

3 Direct piezoelectric actuators

Direct piezoelectric actuators use piezoelectric materials in a relatively straightforward path. This big class is divided according to structural design: unimorph, bimorph, and amplified schemes.

3.1 Unimorph piezoelectric actuators

The typical structure of a unimorph piezoelectric actuator is a single layer of a piezoelectric material sandwiched by two thin conductive metal electrode layers [67–69], and the actuator is usually bonded onto an elastic structure, such as an elastic shim [70].

Unimorph piezoelectric actuators can be divided according to shape: square/rectangular, ring, circular, and cantilever types [71]. They can also be divided according to the working mode: bending mode, linear expansion/retraction mode, etc., as shown in Figs. 4(a)–4(c). The main piezo coupling coefficient in the adopted operating methods is d_{31} (transversal mode).

Figure 5 [72–78] presents various unimorph actuators. Most representative unimorph actuators are the RAINBOW (reduced and internally biased oxide wafer) [72,79] and THUNDER (thin layer unimorph driver) [73,80] actuators, as shown in Figs. 5(a) and 5(b). The introduced prestressing and arching help to produce greater displacement [81,82]. Typical applications of unimorph actuators include fish-shaped robot [74] (Fig. 5(c)), cooling fan [75] (Fig. 5(d)), active vibration isolation system [76] (Fig. 5(e)), multi-DOF micromanipulator [77] (Fig. 5(f)), miniature underwater robot [78] (Fig. 5(g)), proportional microvalve [83], etc. Another application of unimorph actuators focuses on piezoelectric micromachined ultrasound transducers (PMUTs), which mainly utilize their vibration characteristics [84]. In the commercial field, three major companies have researched them: Qualcomm has developed the first commercialized in-display 3D sonic sensor for map 3D fingerprints (Fig. 5(i)). TDK Inc. commercialized rangefinders that can be used for 1.2 and 5 m ranges, respectively (Fig. 5(h)). Exo Inc. achieved a handheld prototype of a PMUT array, consisting of 4096 low-power units, for multiharmonic imaging (Fig. 5(j)).

Unimorph piezoelectric actuators, in terms of their deformable structure, are the simplest and most primitive type. Therefore, theoretically, their deformable parts hold the advantages of excellent reliability and repeatability in terms of the actuating mechanism, while these characteristics also lead to the disadvantages of short stroke [10] and weak load capacity. The latter has the same effect on its overall structure in actual use.

3.2 Bimorph piezoelectric actuators

Bimorph piezoelectric actuators usually consist of two layers of piezoelectric materials with or without metal shim. The asymmetric expansion of the piezoelectric material along its length brings up amplified bending effects and larger tip displacements [70], while the demerit incorporates weak load capacity [85,86]. As listed in Fig. 6(a), the main operation modes and structure classification are roughly the same as those of unimorph piezoelectric actuators. The electrical connections of the piezoelectric layers in the bimorph actuators are different and have two configuration modes: parallel and antiparallel [9]. The former means that the polarization directions of the two piezoelectric layers are the same, while the latter means that they are configured with opposite polarization directions [87,88], as shown in Figs. 6(b) and 6(c). The tip displacement of the antiparallel configuration is usually smaller than that of the parallel configuration mode [89] because the deformation of different PZT layers of antiparallel is opposite, resulting in a decrease in tip deflection.

Figure 7 [90–93] shows some applications of bimorph piezoelectric actuators. Similar to unimorph piezoelectric actuators, bimorph piezoelectric actuators have made great strides and found applications in many fields, but they occupy a large proportion in the fields of robotics and automation, such as robotic assembly [90] (Fig. 7(a)), microgripper [91] (Fig. 7(c)), flipping wing of micro air vehicle [92] (Fig. 7(b)), and insect-scale robots [93] (Fig. 7(d)). In addition, the materials used are expanded to PZT, PVDF [94,95], ZnO [96,97], and other novel piezoelectric materials [98,99].

In summary, bimorph piezoelectric actuators are a structural improvement of the unimorph piezoelectric actuators with the consequent benefits of larger tip displacement, more reliable overall construction, and stronger output force. These features also expand the scope of the application.

3.3 Amplified piezoelectric actuators

3.3.1 Multiple piezoelectric stack actuator (PSA)

The deformation of a single-layer piezoelectric material is usually small because of the limited thickness of a single layer [100,101]. Researchers and engineers explored many avenues to increase the deformation, and one of the easiest ways is to stack up multiple layers whose deformation orientations are identical (called “piezostack”). The stacking strategy can amplify the deformation and driving force. This kind of actuator usually has a large blocking force [102], which refers to the maximum static

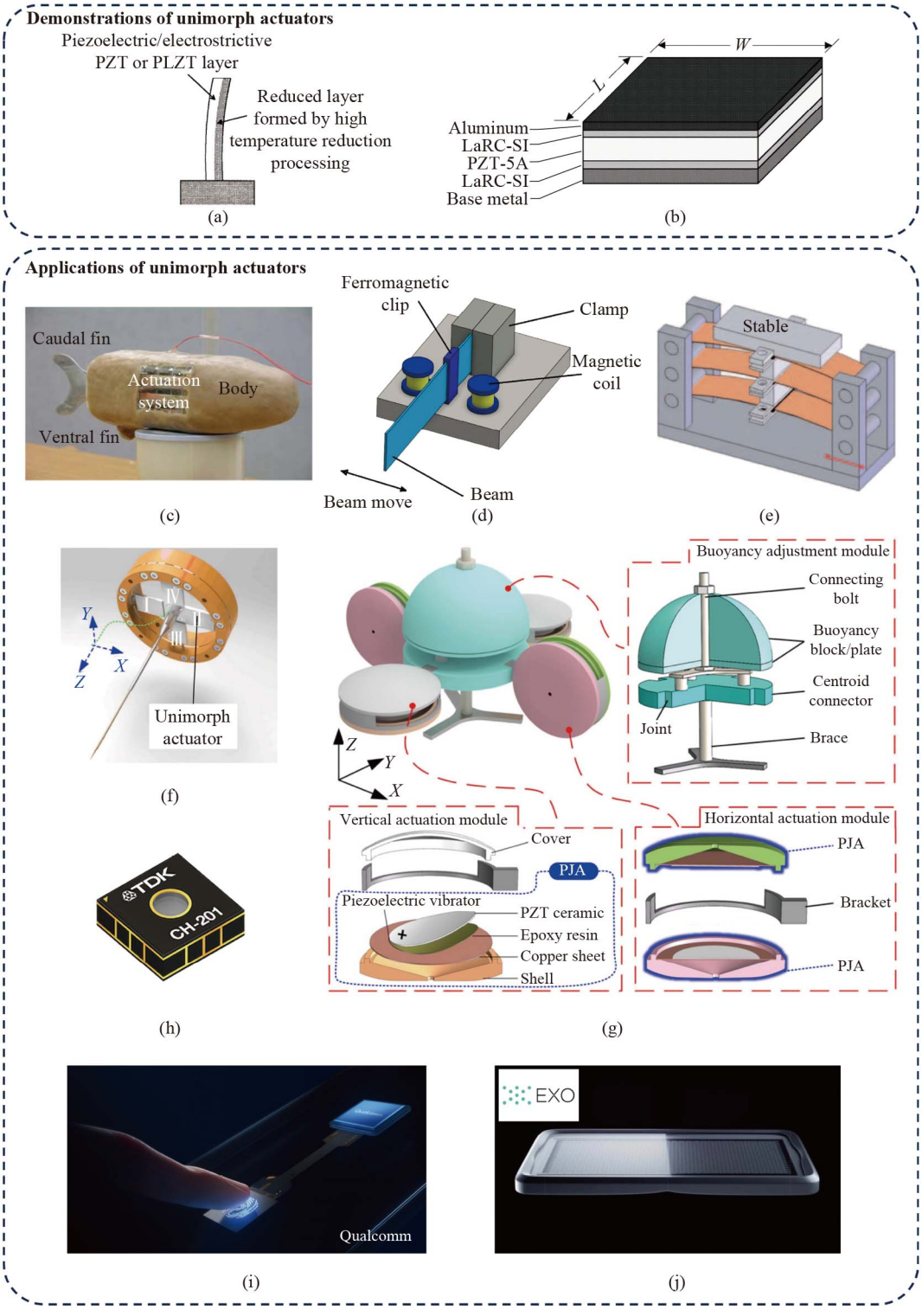

Fig. 5 Different kinds of unimorph piezoelectric actuators and applications: (a) RAINBOW actuator [72], reproduced with permission from AIP Publishing; (b) THUNDER composite laminate [73], reproduced with permission from SPIE; (c) biomimetic fish-shaped robot [74], reproduced with permission from Springer Nature; (d) piezo cooling fan [75], reproduced with permission from Elsevier; (e) active vibration isolation system [76], reproduced with permission from SAGE Publications; (f) multi-degree of freedom piezoelectric micromanipulator [77], reproduced with permission from IEEE; (g) miniature cross-shaped underwater robot [78], reproduced with permission from IEEE; (h) CH201, a 5 m piezoelectric micromachined ultrasound transducer rangefinder commercialized by TDK Inc., reproduced with permission from IEEE; (i) 3D sonic sensor used as an in-display fingerprint sensor developed by Qualcomm Inc., and (j) Cello, a handheld portable piezoelectric micromachined ultrasound transducer-based imaging probe developed by Exo Inc. PJA: pulsed-jet actuator, PZT (PLZT): piezoelectric lead zirconate titanate.

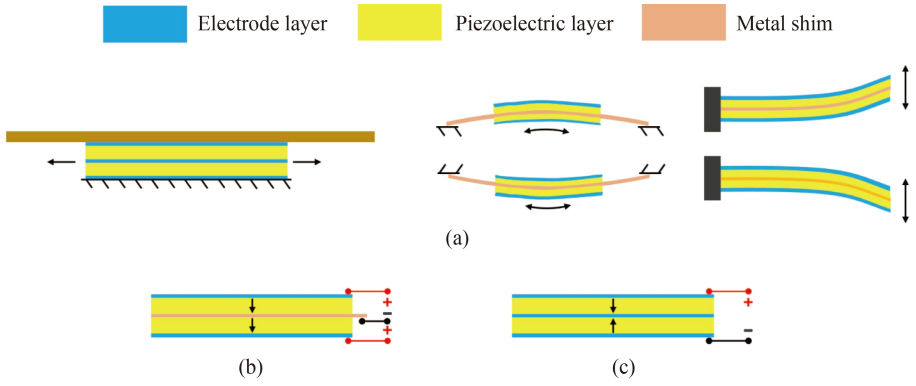

Fig. 6 Bimorph piezoelectric actuators: (a) linear expansion/retraction mode and bending mode, (b) parallel configuration, and (c) antiparallel configuration.

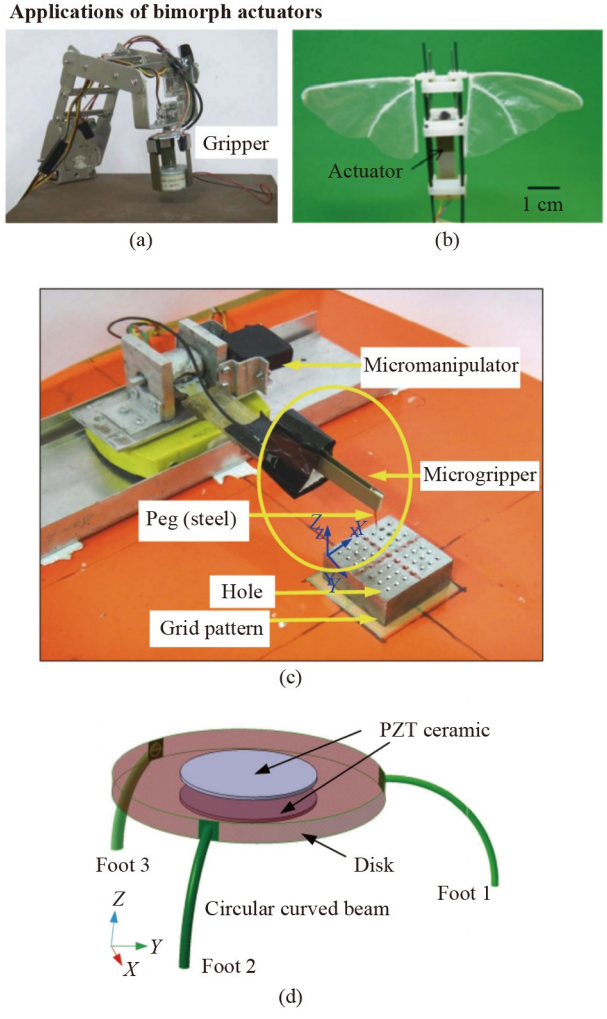

Fig. 7 Use of bimorph piezoelectric actuators in different scenarios: (a) prototype of the bimorph actuator-based manipulator arm [90], reproduced with permission from SAGE Publications; (b) flapping micro air vehicle [92], reproduced with permission from Springer Nature; (c) piezoelectric actuator-based microgripper [91], reproduced with permission from SPIE; and (d) insect-scale robots [93], reproduced with permission from IEEE. PZT: piezoelectric lead zirconate titanate.

compressive strength that can be applied to the actuator without causing permanent damage or failure.

Figure 8 shows three stacking methods, namely, longitudinal stacking, transversal stacking, and shear stacking. The corresponding piezoelectric coupling coefficients are d_{33}, d_{31}, and d_{15}, respectively.

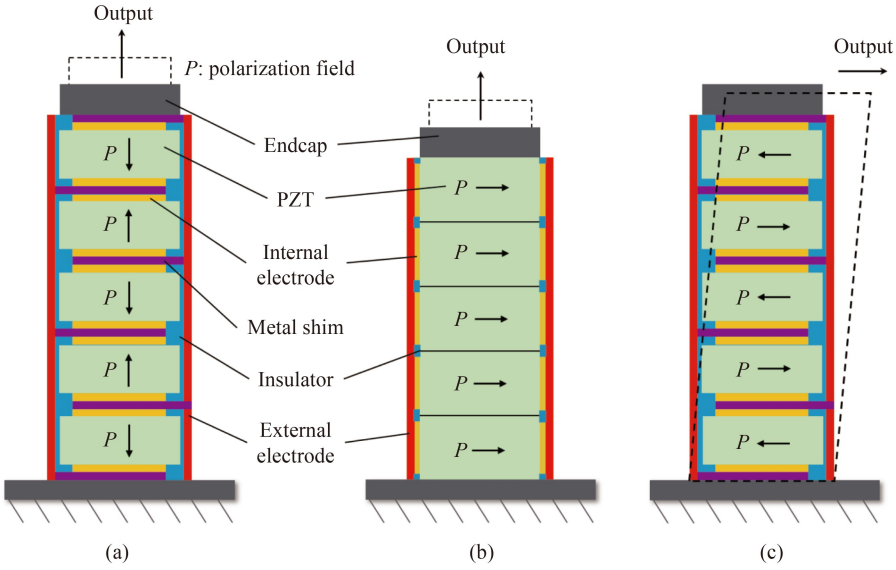

Fig. 8 Three structures of the stack: (a) longitudinal stack, (b) transversal stack, and (c) shear stack. PZT: piezoelectric lead zirconate titanate.

In a longitudinal stack, as shown in Fig. 8(a), the polarization directions of two adjacent layers are opposite, and the internal electrodes of the same polarity are connected through the metal shim in the middle. The stack is powered by two external electrodes, driving the multiple layers simultaneously. The transversal stack and the shear stack, as shown in Figs. 8(b) and 8(c), hold the same electrical connections by locating the internal electrodes of the same polarity on the same side of a layer of piezoelectric material, while the distribution of polarization orientation of each layer is different.

The output displacements for three stacking modes with n layers of piezoelectric materials can be expressed as

$$L_{\mathrm{l}} = nd_{33}U, \tag{1}$$

$$L_{\mathrm{t}} = nd_{31}\frac{Ul}{h}, \tag{2}$$

$$L_{\mathrm{s}} = nd_{15}U, \tag{3}$$

where L represents the output displacement, whose subscript represents the corresponding stacking mode, U is the voltage applied to the external electrodes, and l and h represent the length and height of the single layer of piezoelectric material, respectively.

Piezostack is a mainstream product of direct piezoelectric actuators. Table 4 lists typical models of mature products supplied by large corporations. It outlines the performance parameters, including operating voltage, temperature, and blocking force, which can help achieve a general understanding and choose the feasible product on demand. Notably, the accuracy of the stack products is not listed here because it is affected by many factors, such as the actuator size and the resolution of the signal controller, which cannot be quantified in a unified standard.

PSAs, especially the longitudinal stack and shear stack, can have different shapes [103–105] and external electrode settings [106]. Piezostacks incorporate the

Table 4 Piezo stack products from different companies

Affiliated company	Product	Main feature	Operating voltage/V	Operating temperature/°C	Blocking force/kN
Physik instrumente (PI)	P-007–P-056 PICA stack piezoelectric actuators	High forces up to 78 kN, high displacement up to 300 μm, flexible production	0–1000	−20–85	0.65–78.00
	P-080 PICMA stack multilayer ring actuators	With an inner hole for preload or an aperture for optical applications, ideal for dynamic operation	−20–100	−40–150	0.80–0.85
	P-088 round PICMA stack multilayer piezoelectric actuators	High blocking force up to 7.5 kN, flexible and adaptable overall height	−20–100	−40–150	7.50
Piezo direct	PDJ150 series for rectangular actuators	–	−20–150	−20–120	0.25–7.20
	PDH200 series for ring actuators	–	−20–200	−20–120	3.60–7.20
Cedrat technologies	Parallel pre-stressed actuator series	Low voltage piezo ceramic, optimal preload for high dynamics	−20–150	–	1.10–9.30
COREMORROW	NAC20 series	–	0–60, 150, 200	0–150	0.17–9.45
	NAC21 series	–	0–60, 150, 200	0–150	1.06–8.45

merits of larger stroke, large blocking force, low actuating voltage, and rapid response, while the demerits include possible large size and weak resistance to tensile deformation [9,107,108].

3.3.2 Piezoelectric actuators with flexible hinges

Another type of amplified piezoelectric actuator is flexible hinge based [109], wherein flexible hinges are made of elastic materials, and the whole structure contains no assembly components. From the perspective of structure, this type of actuator can be further divided into three categories: lever-type amplification mechanism (LAM), triangular-type amplification mechanism (TAM), and hybrid-type amplification mechanism (HAM) [13, 110]. Figures 9 and 10 show different types of flexible hinges and respective equivalent models. When in use, the elastic part deforms under the force generated by the piezoelectric actuator unit and releases amplified displacement through the predesigned structure.

Figure 11 [111–114] shows typical structures based on LAM and TAM. Multiple functions can be realized by LAM-based actuators. As shown in Figs. 11(a) and 11(b), a simple two-DOF microgripper with a grip and rotation range of 50–500 μm was proposed by Dsouza et al. [111]. Wu et al. [115] used this structure to drive the chopper mirror and realized a displacement amplification ratio of 9. TAM-based actuators, which contain the bridge type, can also be used in various applications, such as tripod manipulation [116], miniature gripping [112] (Fig. 11(c)), and simple displacement amplification [117]. Juuti et al. [118] combined prestressed and bridge-amplified structures to construct an enhanced piezoelectric displacement actuator. The Scott–Russell (S–R)-type flexible hinge has the characteristic where the output displacement is a straight line under a given input. A typical demonstration is the symmetrical microgripper designed by Sun et al. [113], which has a jaw displacement of 134 μm and an amplification ratio of 15.5 (Fig. 11(d)). Tian et al. [114] designed a piezoelectric actuator for nanomanipulation (Fig. 11(e)). In addition, the micropositioning platform based on this structure can be used to identify the S–R mechanism driven by the piezoelectric actuator [119].

In summary, piezoelectric actuators with flexible hinges have the advantages of compact structure, smooth and repeatable motion, low inertial mass, low wear, and

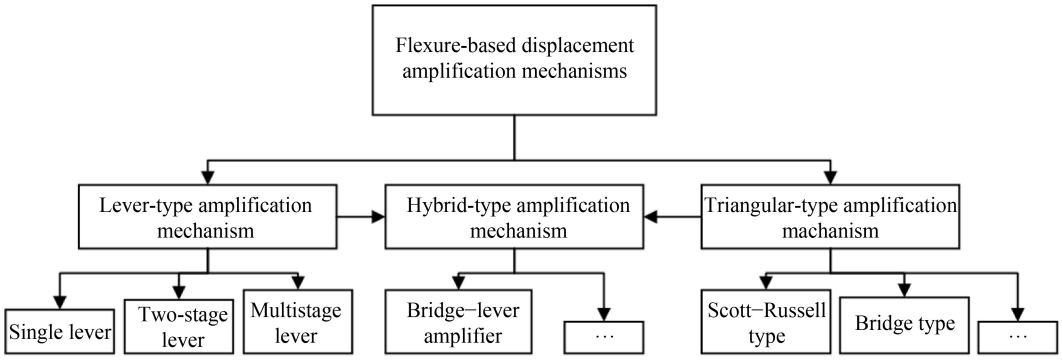

Fig. 9 Classification of flexible hinges.

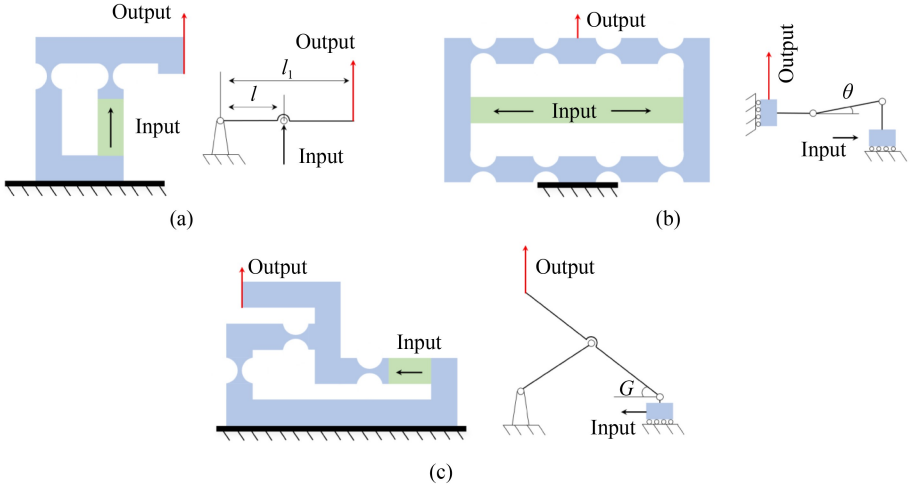

Fig. 10 Amplification mechanism using flexible hinges: (a) single lever type, (b) bridge type, and (c) Scott–Russell type.

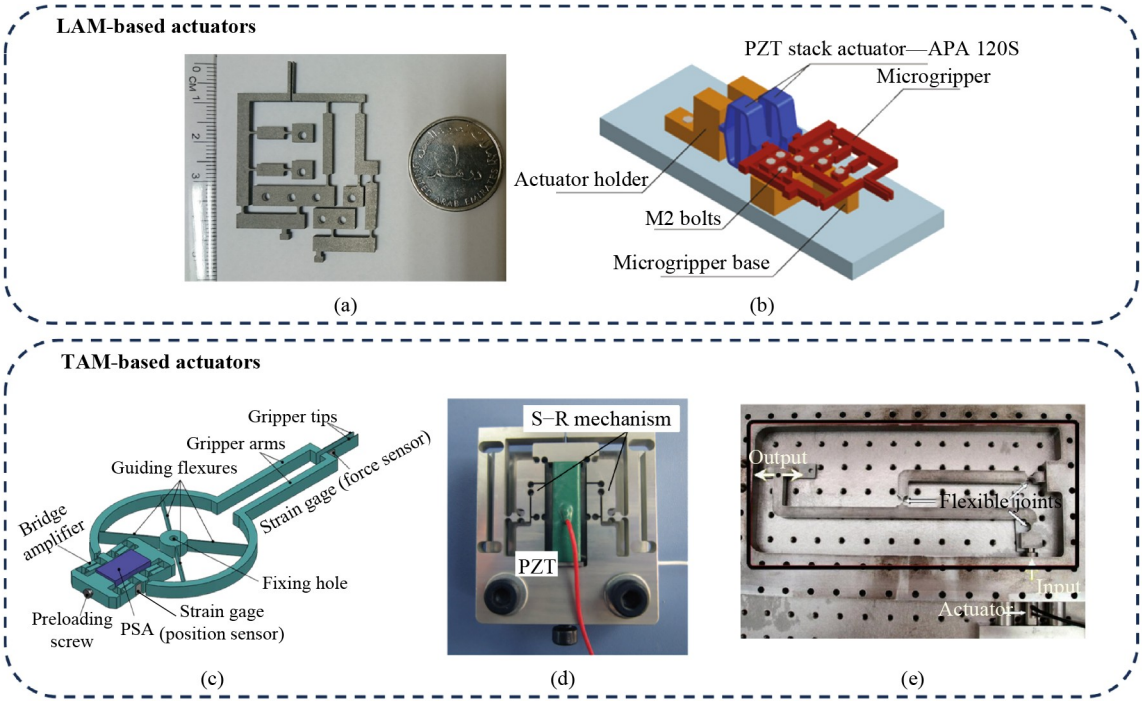

Fig. 11 Piezoelectric actuators with a flexible hinge mechanism: (a) size comparison of the fabricated microgripper of lever type with piezoelectric actuator and (b) CAD model of the microgripper [111], reproduced with permission from Springer Nature; (c) CAD model of the miniature gripper of bridge type [112], reproduced with permission from IEEE; (d) prototype of the piezo actuator with a Scott–Russell (S–R) flexible hinge [113], reproduced with permission from AIP Publishing; and (e) photo of the flexure-based S–R mechanism for nanomanipulation [114], reproduced with permission from Elsevier. LAM: lever-type amplification mechanism, PSA: piezoelectric stack actuator, PZT: piezoelectric lead zirconate titanate, TAM: triangular-type amplification mechanism.

no "backlash" phenomenon. The disadvantages include weak output torque, poor overall stiffness, easy breakage due to stress concentration, and relatively slow response speed.

4 Indirect piezoelectric actuators

Contrary to direct piezoelectric actuators, indirect piezoelectric actuators use relatively complex structures to output displacement, which can be subdivided into ultrasonic motors and stepping actuators, in terms of the output displacement mode. From a principal point of view, the latter ones contain friction–inertia actuators and stick–slip actuators, as shown in Fig. 2.

4.1 Ultrasonic actuators

Ultrasonic piezoelectric actuators are known as ultrasonic motors. Although this type of actuator can realize stepping motion, in principle, it is essentially different from the stepping actuators. Current ultrasonic motors stem from the research conducted by Japanese Scientist Sashida in 1982 and 1983 [120,121]. Ultrasonic motors can be divided into standing wave ultrasonic, traveling wave ultrasonic, and hybrid-mode motors [122] in terms of the type of driving mode [123,124]. They can be classified into single-DOF motors and multi-DOF motors from another perspective. The advantages include high speed and torque, fast response, ease of miniaturizing, quiet operation, antielectromagnetic interference, and no "backlash" phenomenon, while the disadvantages include complicated structure and control system, and reduced working life due to potential running heat [125].

The key point to the operation of standing and traveling ultrasonic motors is the elliptical motion of the driving foot relative to the rotor. As shown in Fig. 12, the process can be expressed as follows: The piezoelectric material excites the microvibration of the stator, an elastic body, above the ultrasonic frequency (> 20 kHz), and then the vibration is amplified by the resonance of the stator and transformed into the rotational/linear motion of the rotor through the friction movement between the stator and rotor. In addition to the working principle mentioned above, new varieties have emerged. Readers who are interested in ultrasonic motors can further refer to relevant reviews [19,126]. In consideration of the focus of this review, the next sections will only discuss the most common standing wave ultrasonic motors and traveling wave ultrasonic motors in detail.

4.1.1 Standing wave

As the name suggests, a standing wave motor (SWM)

generates the elliptical motion of the driving foot through the standing wave excited by the stator, as shown in Fig. 13(a). Specifically, standing waves are excited as follows: A driving source is placed in a closed loop (round or square), and the driving source works at the resonant frequency of the loop; then, the standing wave is generated when two symmetrically propagated vibration waves superimpose with each other [123]. The standing wave has the following expression:

$$y(x,t) = A\cos(kx)\cos(\omega t), \tag{4}$$

where t and ω are time and angular frequency, respectively, A represents the amplitude of the standing wave, k is the wavenumber whose value is equal to $2\pi/\lambda$ (λ is the wavelength of the standing wave), and the coordinate of a certain position on the elastic body is represented by x. The motion direction of the rotor is determined by the vibration direction of the driving foot, as shown in Figs. 13(b) and 13(c). If the trajectory of the driving foot is from bottom-left to top-right, then the rotor moves to the right, and vice versa.

SWM can be divided into linear SWMs and rotary SWMs according to the displacement output form, whereas they can be unidirectional SWMs and bidirectional SWMs [127] according to displacement direction. Figure 14 [128–137] shows various types of SWMs and their applications. In the structure shown in Fig. 14(a), Wang et al. [128] designed an asymmetric linear SWM and achieved a speed of 127.31 mm/s. The longitudinal bending coupled motor proposed by Liu et al. [129] went one step further, pushing forward the speed to 891.3 mm/s (Fig. 14(b)). Fan et al. [138] improved the thrust–weight ratio of this type of motor by signal control. An SWM applicable to special circumstances, such as the deep sea, proposed by He et al. [130], can achieve a speed of 214 mm/s underwater at a pressure of 8 MPa (Fig. 14(c)). Jian et al. [131] designed a linear ultrasonic motor to meet the requirements of an absolute gravimeter (Fig. 14(i)). Yeh et al. [132] used ultrasonic motors in a haptic feedback system to improve medical devices' haptic perception and operation ability (Fig. 14(j)). In addition, this type of motor can have different shapes for different

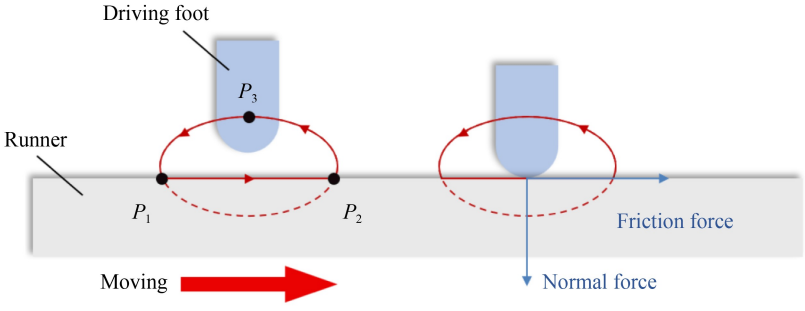

Fig. 12 Basic operating principle of the ultrasonic piezoelectric actuators.

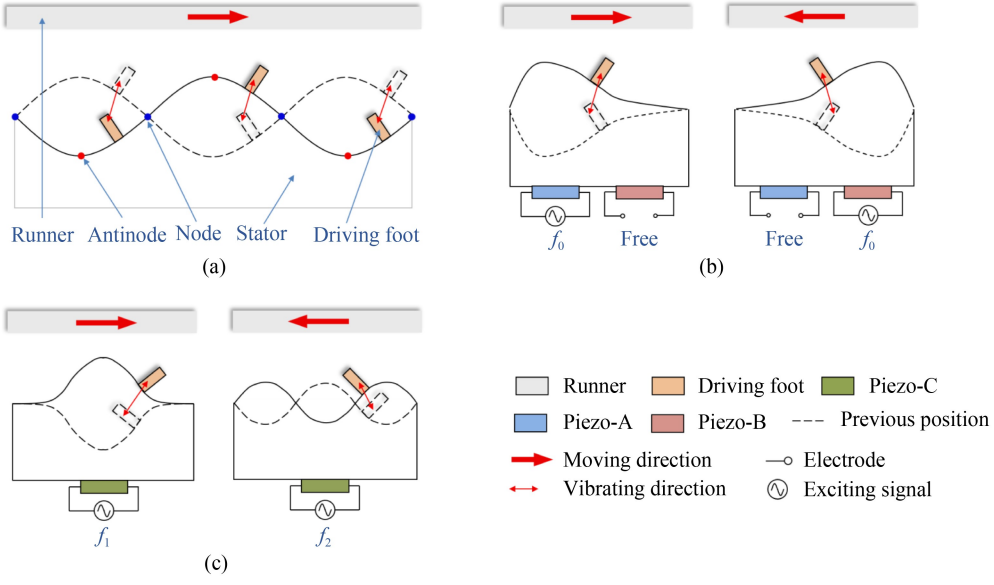

Fig. 13 Excitation of standing waves and methods of changing direction: (a) operating principle of standing wave motor, changing the propagation direction by (b) electrode configuration and (c) frequency configuration.

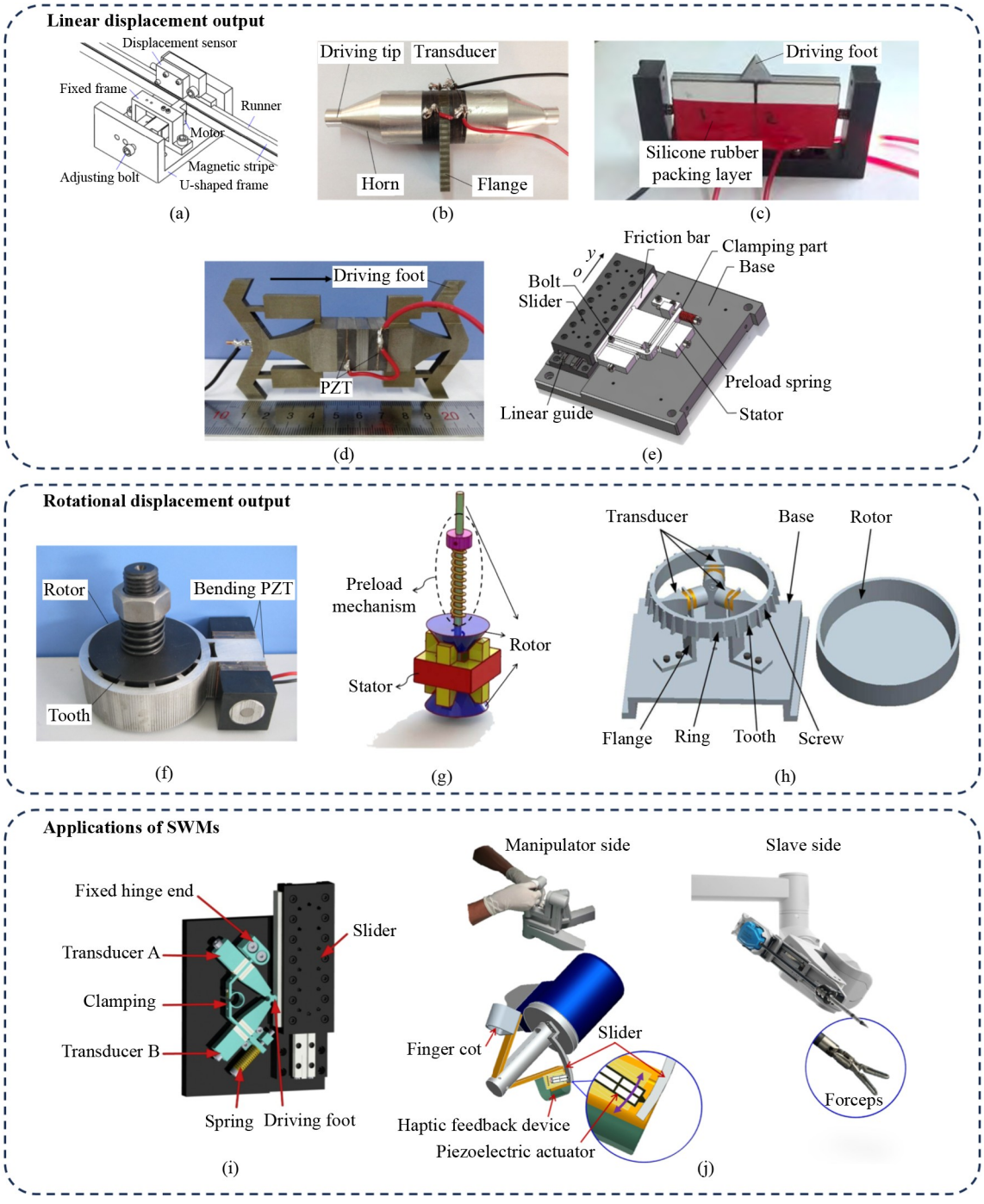

Fig. 14 Various standing wave ultrasonic motors: (a) prototype of the linear ultrasonic motor based on asymmetric structure [128], reproduced with permission from Elsevier; (b) actuator prototype proposed by Liu et al. [129], reproduced with permission from Elsevier; (c) actuator used for deep sea [130], reproduced under the terms of the CC BY license; (d) prototype of the frog-shaped ultrasonic actuator [133], reproduced with permission from IEEE; (e) L-shaped ultrasonic motor [134], reproduced with permission from AIP Publishing; (f) standing wave ultrasonic motor with rotational displacement output [135], reproduced with permission from Elsevier; (g) bidirectional ultrasonic motors [137], reproduced with permission from Elsevier; (h) standing wave ultrasonic motor with three transducers [136], reproduced with permission from Trans Tech Publications; (i) ultrasonic motor for absolute gravimeter [131], reproduced with permission from Elsevier; and (j) ultrasonic motor for haptic feedback [132], reproduced with permission from Elsevier. PZT: piezoelectric lead zirconate titanate, SWM: standing wave motor.

applications, such as frog-shaped [133] (Fig. 14(d)), L-shaped [134] (Fig. 14(e)), and trapezoidal [139].

Rotary SWMs also have an extensive range of applications. Liu et al. [135] realized a prototype with a

typical no-load output speed of 165 r/min and maximum torque of 0.45 N·m at a sinusoidal input peak voltage of 282 V and a frequency of 28.17 kHz as shown in Fig. 14(f). Recently, Liu et al. [136] presented a prototype of a rotary SWM with three longitudinal vibration transducers (Fig. 14(h)). The aforementioned two types of motors have unidirectional [140,141] and bidirectional [135,137] (Figs. 14(f) and 14(g)) modes according to the direction of the output displacement.

In general, SWMs exhibit features of low cost and high efficiency due to the few driving sources, while the standing wave scheme causes more wear and tear compared with traveling wave-based motors [19,142].

4.1.2 Traveling wave

The difference between the traveling wave motor (TWM) and the SWM is that the elliptical motion of the driving foot does not come from fixed points but from all points of the contact surface of the stator. Specifically, two standing waves with the same amplitude and frequency but a spatial difference of a quarter wavelength and a phase difference of π/2 in time [19] can synthesize a traveling wave. The synthetic traveling wave propagates in the opposite direction to the elliptical [143], as shown in Fig. 15.

Equations (5) and (6) are the expressions of two standing waves, and Eq. (7) represents the synthetic traveling waves.

$$y_1(x,t) = A\sin\left(\frac{2\pi}{\lambda}x\right)\cos(\omega t), \tag{5}$$

$$y_2(x,t) = A\sin\left(\frac{2\pi}{\lambda}\left(x+\frac{\lambda}{4}\right)\right)\cos\left(\omega t+\frac{\pi}{2}\right), \tag{6}$$

$$y_3(x,t) = y_1 + y_2 = A\sin\left(\frac{2\pi}{\lambda}x-\omega t\right). \tag{7}$$

Figure 16 [144–150] shows different kinds of TWMs and their applications. Many studies have been conducted on TWMs. In the structure shown in Fig. 16(a), Chen et al. [144] proposed a typical TWM utilizing a radial bending of a thick ring and finally achieved a maximum speed of 146 r/min and torque of 1 N·m. Sun et al. [145] combined the preload optimization method and thus designed a TWM-based cooperative manipulator applicable to the industrial field (Fig. 16(e)). Jia et al. [146] applied the TWM to wheeled robots and achieved a no-load maximum speed of 136.8 mm/s (Fig. 16(d)). TWMs can be used as vibration feeding devices [147] (Fig. 16(g)), and they have been widely used in camera focusing systems [148,151] (Fig. 16(f)), aerospace, biological equipment, etc. [152], wherein this kind of motor can have different designs, including spherical [149,153] (Fig. 16(b)), cylindrical [154], hollow [150,155] (Fig. 16(c)), arc-shaped [156], etc. In the future, improving the performance of TWMs will be a subject of continuing interest [157].

TWMs can easily realize forward and backward movement, thus offering great design and usage flexibility. The potential disadvantage is that the operation efficiency is reduced due to the requirement of multiple signal-generating sources to generate the driving signal. The complex structure and the difficulty of miniaturization also restrict its application.

4.2 Stepping actuators

Stepping actuators drive moving components and output displacement step by step. This method effectively addresses the shortcoming of short strokes for traditional piezoelectric actuators. Stepping actuators can be classified into friction inertial, inchworm, and other forms [158]. The first two forms are discussed in detail in this section.

4.2.1 Friction–inertia actuators

The fundamental principle of friction–inertia actuators is

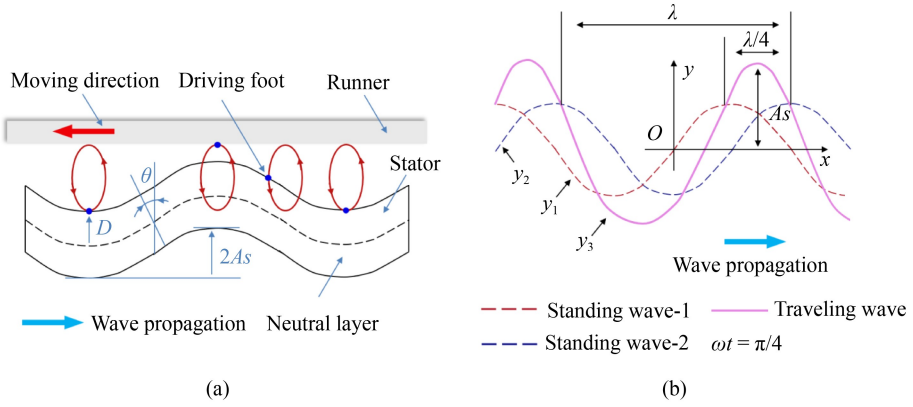

Fig. 15 Operating principle of the propagating wave motor: (a) elliptical motion of the driving feet and (b) synthesis of the propagating wave.

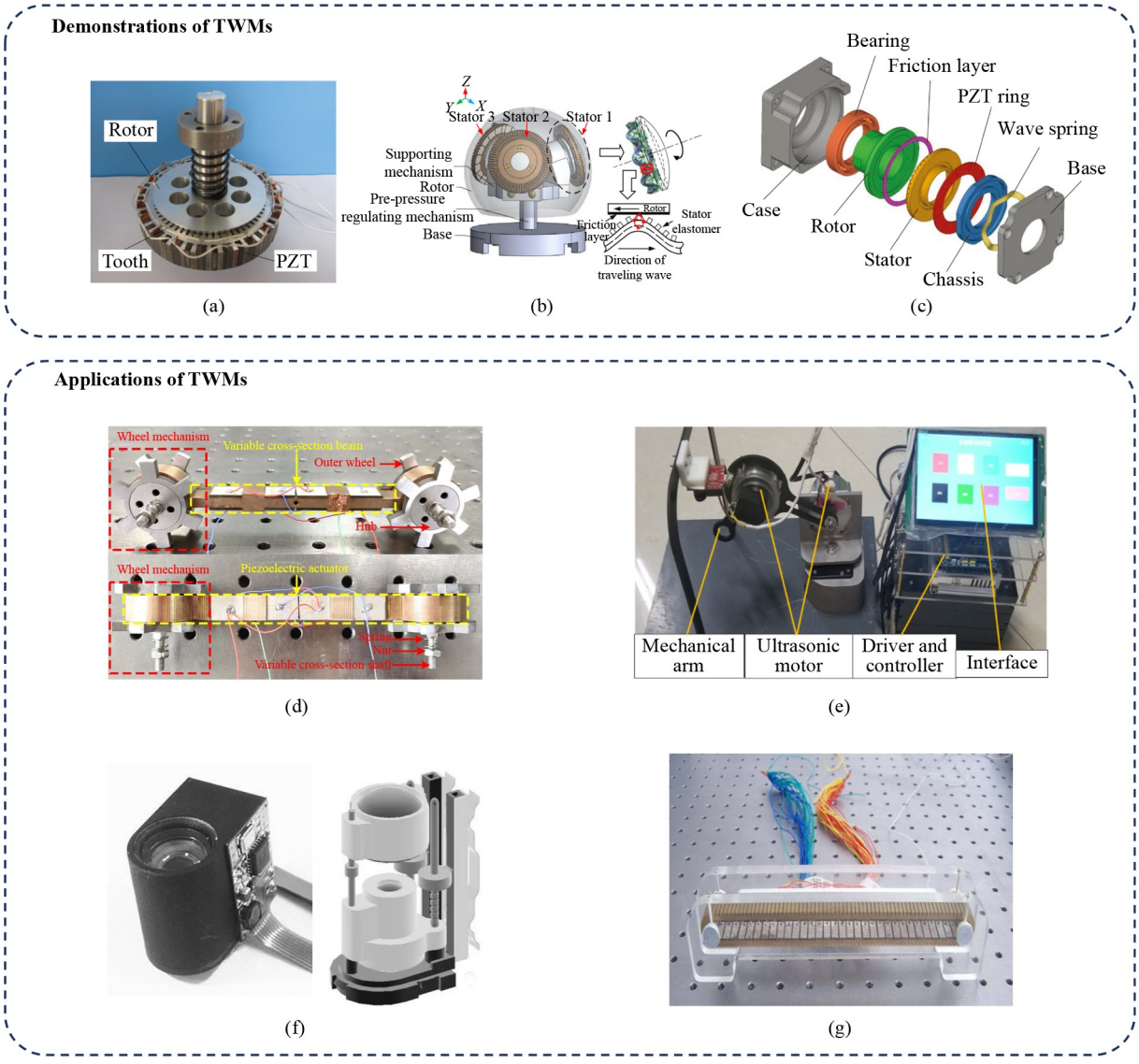

Fig. 16 Various traveling wave ultrasonic motors: (a) prototype ring-type motor with radial bending mode [144], reproduced with permission from IEEE; (b) structure of ball-type multi-degree of freedom motor [149], reproduced with permission from Elsevier; (c) structure diagram of hollow traveling wave rotary motor [150], reproduced with permission from SAGE Publications; (d) traveling wave motor (TWM) for wheeled robot [146], reproduced with permission from IOP Publishing; (e) traveling wave motor for manipulator [145], reproduced under the terms of the CC BY license; (f) traveling wave motor for camera auto zooming of a Samsung cellular phone; and (g) ultrasonic motor for feeding device [147], reproduced under the terms of the CC BY license. PZT: piezoelectric lead zirconate titanate.

the conservation of momentum [159]. The form of the driving signal includes the sawtooth wave, the isosceles triangle wave, the square wave signal, etc. (Fig. 17). Friction–inertia actuators can be divided into inertia/impact drive actuators (IDAs), stick–slip [160] drive actuators (SSDAs), and smooth impact drive actuators [161]. As shown in Fig. 18(a), the simplified model of an IDA consists of two masses and one piezoelectric element. IDAs have a relatively faster-moving speed and less wear than SSDAs, while the mass transport capacity of IDAs must be improved. The displacement of IDAs is generated when the input voltage drops rapidly, and the displacement cycle contains three steps: 1) All components are in the initial state with no external electrical signal. 2) The piezoelectric element expands slowly with the increase in the external input signal. The inertial mass moves to the right while the rest of the system remains stationary. 3) The input electrical signal decreases rapidly, causing the piezoelectric element to contract rapidly. Given that the inertial impact force is greater than the static friction, the main block moves to the right with the distance Δs. By repeating the above steps, IDAs can realize unrestricted stroke.

Figure 19 [162–166] shows two different displacement

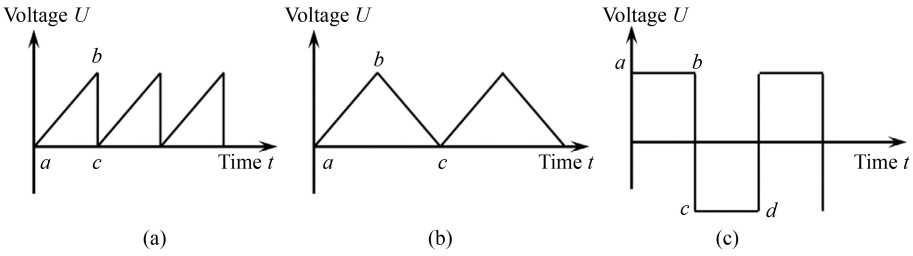

Fig. 17 Different control signals for friction–inertia actuators: (a) sawtooth wave signal, (b) isosceles triangle signal, and (c) square wave signal.

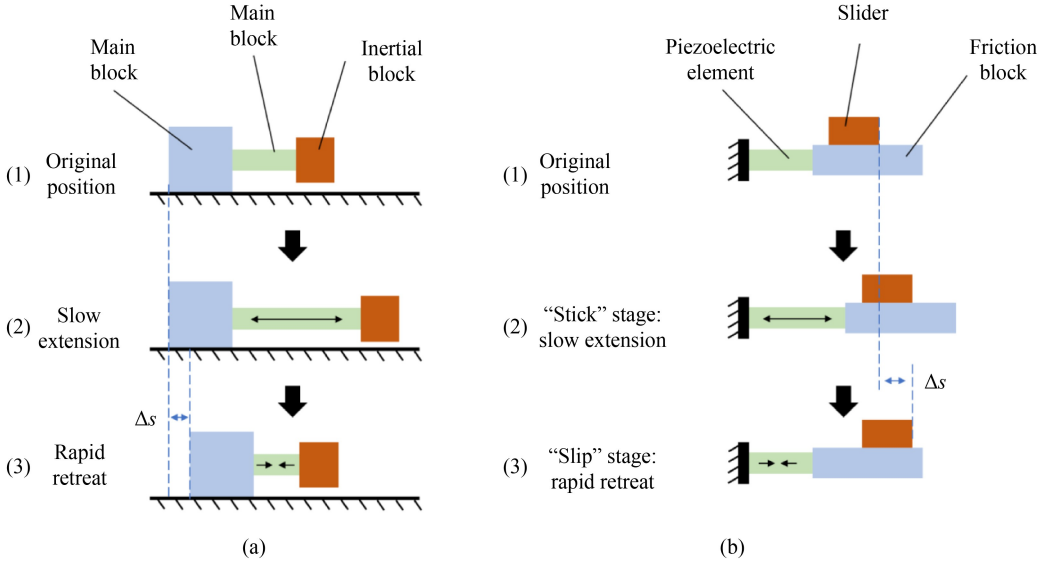

Fig. 18 Actuating principles of friction–inertia actuators: (a) principle of inertia/impact drive actuator and (b) principle of stick–slip drive actuator.

output methods of IDA, including linear displacement output and rotational displacement output. IDAs have found vast applications in various fields. A typical application is the positioning platform [159]. For example, Yamagata et al. [167] designed a hexagon-shaped three-axis positioning table based on IDAs to be employed in an ultrahigh vacuum environment. IDAs can be used for linear drives [162,163,168] (Figs. 19(a) and 19(b)) and rotary drives [164] (Fig. 19(d)). Hua et al. [165] designed a precision linear actuator, whose impact force is generated by a set of asymmetrically clamped cantilever bimorphs, and it achieved a maximum load capacity of larger than 100 g (Fig. 19(c)). A rotary inertial actuator using two piezoelectric stacks as power converters was designed by Wen et al. [166]; this actuator achieved an angular displacement resolution of 10 μrad when driven by a 15 V_{pp} (peak to peak voltage) square wave with a frequency of 10 Hz (Fig. 19(e)).

Different from IDAs, the motion process of an SSDA is smoother, and the output displacement motion is generated when external voltage slowly rises. The transport capacity is relatively better with the cost of more severe wear. The working state of SSDAs includes three steps, as shown in Fig. 18(b):

1) All components are in the initial state without an external electrical signal.

2) The "stick" stage: The piezoelectric element expands gradually with the slow increase in external signal.

3) The "slip" stage: The slider turns back to the original position approximately due to inertia with a rapid decrease in external signal.

The slider changes the position of Δs in one cycle, and the travel can be theoretically unlimited by repeating the above steps.

Figure 20 [169–172] shows various types of SSDAs. After being raised in 1999 [173], SSDAs have been used in medical equipment [169,174] (Fig. 20(a)), robotics [170] (Fig. 20(b)), zoom lenses [175], and other fields in terms of the capability of linear displacement output [171, 176] (Fig. 20(c)) and rotational displacement output [172] (Fig. 20(d)). In addition, the stick–slip drive form may change from "stick–slip" to "slip–slip" [177,178] with a high-frequency drive signal.

As a friction–inertia type, SSDAs are limited in its application due to the "backlash" phenomenon and small

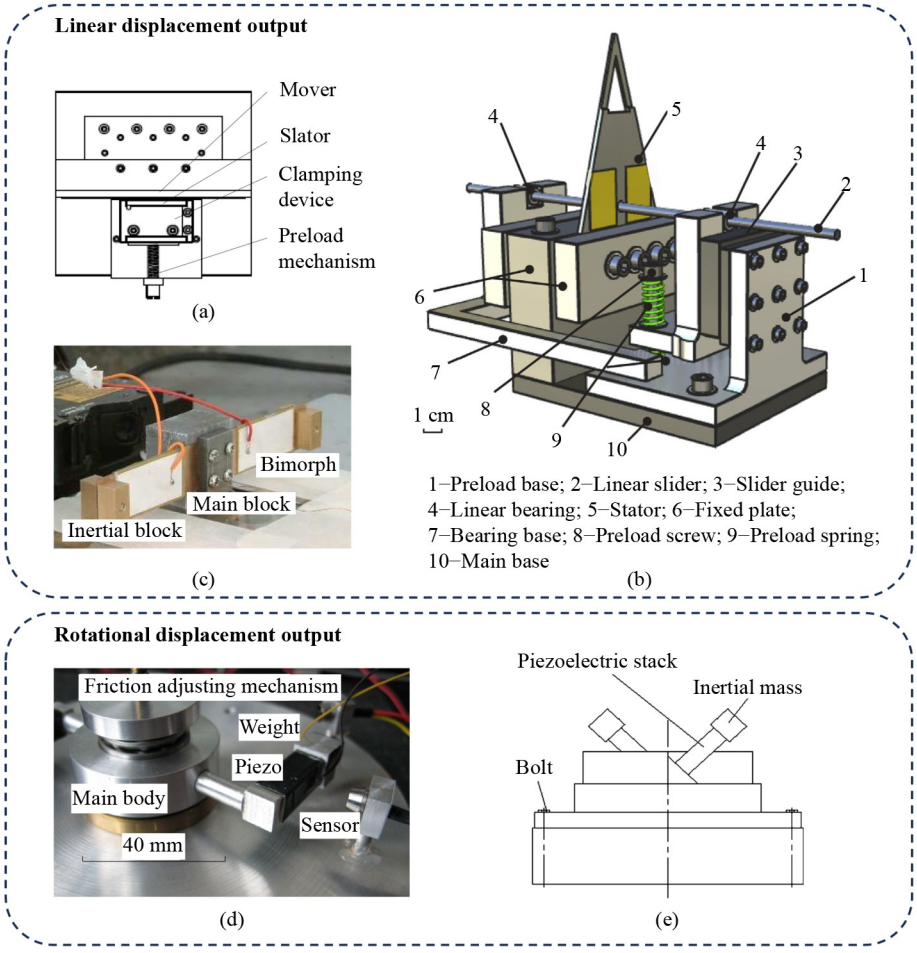

Fig. 19 Different kinds of inertia/impact drive actuators: (a) linear piezoelectric motor by Liu et al. [162], reproduced with permission from Trans Tech Publications; (b) diagram of the prototype by Pan et al. [163], reproduced with permission from Elsevier; (c) prototype of the inertia drive actuator by Hua et al. [165], reproduced with permission from Trans Tech Publications; (d) prototype of rotary piezoelectric motor [164], reproduced with permission from SPIE; and (e) structure of the rotary actuator by Wen et al. [166], reproduced with permission from Springer Nature.

output force. The former not only limits the motion speed, accuracy, and efficiency but also causes the surface abrasion of the slider, reducing the working life. Two methods to deal with this problem are to modify the input signal or improve the mechanical mechanism. Cheng et al. [179] proposed a friction control method based on composite waves to suppress "backlash" phenomenon, and the experimental results show that the "backlash" phenomenon is reduced by 83% and 85%. For individual waveforms and the use of signal modification methods, "backlash" phenomenon has been suppressed, and the output load capacity has been increased on driving signals, such as sawtooth waves [179] and triangle waves [180]. In terms of mechanical structure, Fan et al. [181] proposed a synergic motion principle to suppress this phenomenon by using two piezoelectric stacks to control contact force effectively during actuation. Test results show that under optimal experimental conditions, the actuator could output stepping displacement without backward motion. Recent studies have also reported that using mechanical mechanism and input signals together can suppress the "backlash" phenomenon. Deng et al. [182] designed a bionic quadruped piezoelectric actuator platform, which applied two sawtooth wave exciting signals with a phase difference to suppress this phenomenon and improve the linearity of the output displacement (0.9998 and 0.9999). We believe that the combined use of the above two methods can achieve better improvement effects, and the introduction of a new principle of feedback mechanism, such as magnetic force [183], can push the application of this type to a broader range.

In general, this type of actuator has the advantages of unrestricted travel, a simple control system, and low cost; the disadvantages include slow speed, weak output torque, insufficient transport capacity, accumulated errors, severe wear, and relatively short life span due to the "backlash" phenomenon [10,159].

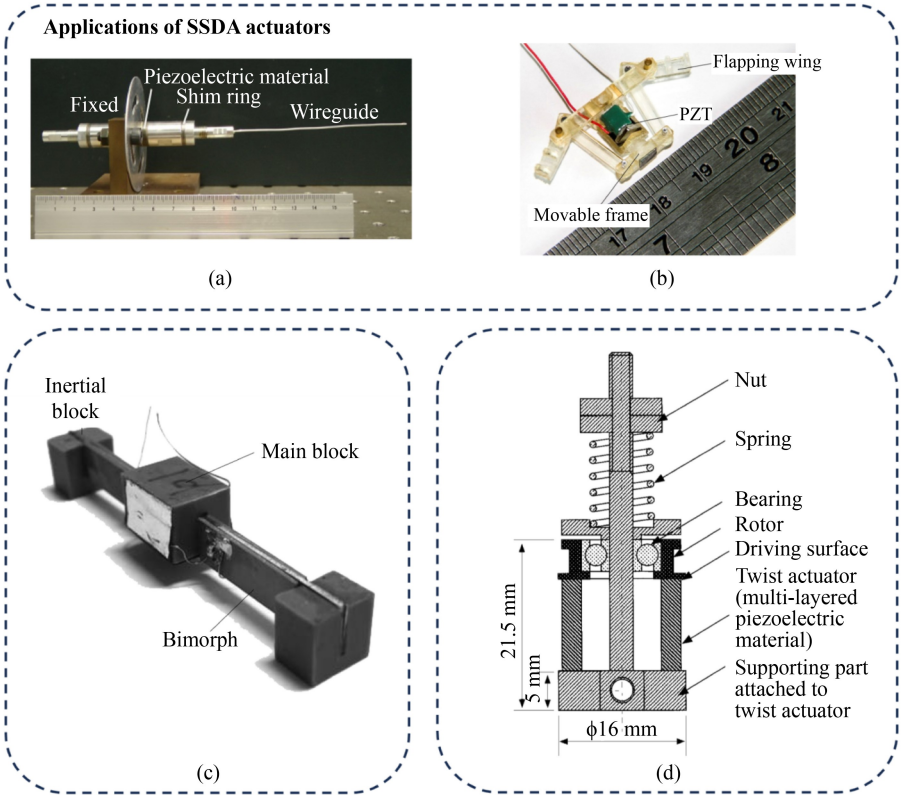

Fig. 20 Different kinds of stick–slip drive actuators (SSDAs): (a) photograph of SSDA used for endoscopic devices [169], reproduced with permission from Elsevier; (b) prototype of SSDA for flapping wing [170], reproduced with permission from Springer Nature; (c) prototype of a linear SSDA [171], reproduced with permission from Taylor & Francis; and (d) cross-section of the rotary SSDA [172], reproduced with permission from IEEE. PZT: piezoelectric lead zirconate titanate.

4.2.2 Inchworm actuators

The inchworm-type piezoelectric actuator is a novel structure inspired by the movement patterns of real inchworms in nature [184,185]. The structure usually includes three parts, namely, two clamping units and one driving unit, as shown in Fig. 21. The clamping units make the actuator obtain improved load capacity, repeatability, and reliability.

This kind of actuator can be divided into two types in terms of movement: walking mode and pushing mode [159,186]. The walking mode includes six steps:

1) All components are in their initial states without input signals.

2) An input signal is applied to the clamping unit 1 so that it expands and contacts the fixing surfaces.

3) The driving unit expands under the input signal, and the deformation is Δs.

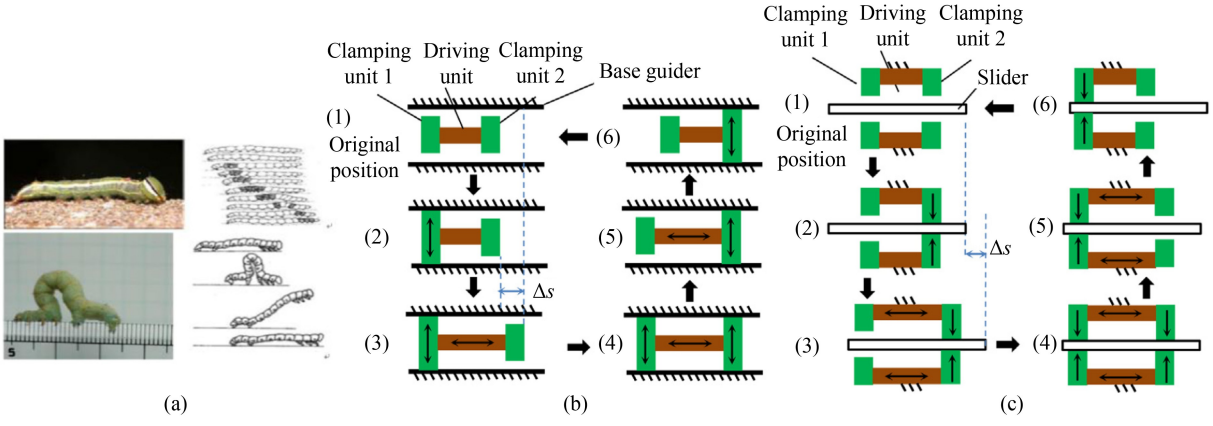

Fig. 21 Motion of inchworm and the operating mode of the actuator [161]: (a) inchworm in nature, (b) walking mode, and (c) pushing mode. Reproduced with permission from Elsevier.

4) Clamping unit 2 contacts the fixed surface under the control of the input signal.

5) Clamping unit 1 returns to the initial state after removing the signal.

6) After removing the signal, the driving unit also returns to the initial state.

The pushing mode is similar and can also be divided into the following six steps:

1) All components are in their initial states without input signals.

2) Clamping unit 2 tightens the slider with the input signal.

3) The driving unit obtains the signal and pushes the slider with a distance of Δs.

4) Clamping unit 1 obtains the input signal and tightens the slider.

5) Clamping unit 2 releases the slider after removing the signal.

6) The driving unit returns to its initial state.

Repeating the above six steps in different modes can obtain unlimited displacement output.

The inchworm piezoelectric actuators were born in the 1960s [187–189], and the general structure of inchworm actuators was proposed by Hsu and Albert [190] in 1966. In the 1980s, this type of actuator gained rapid development due to the production of high-performance piezoelectric elements. Fujimoto [191] first proposed an inchworm actuator with a flexible hinge, and the C-level structure in the prototype improved the clamping force and length of the piezoelectric element. Figure 22 [192–194] presents a series of inchworm actuators incorporating different structures. Kim et al. [192] achieved a magnification ratio of 8.4 at a leverage ratio of 3.6 through a flexible hinge structure (Fig. 22(a)). In addition to flexible hinges, structures, such as wedge blocks, springs [193], and permanent magnets [194], as shown in Figs. 22(b) and 22(c), are used to improve the performance of inchworm piezoelectric actuators.

The current development trend of inchworm piezoelectric actuators is to improve function and structure. Figure 23 [195–199] shows these performance improvements. Function improvements include achieving a large range of high repeatability output steps, multiple DOF, and high speed [195] (Fig. 23(b)), and structure improvements include structure simplification and miniaturization.

Achieving an extensive range of high repeatability

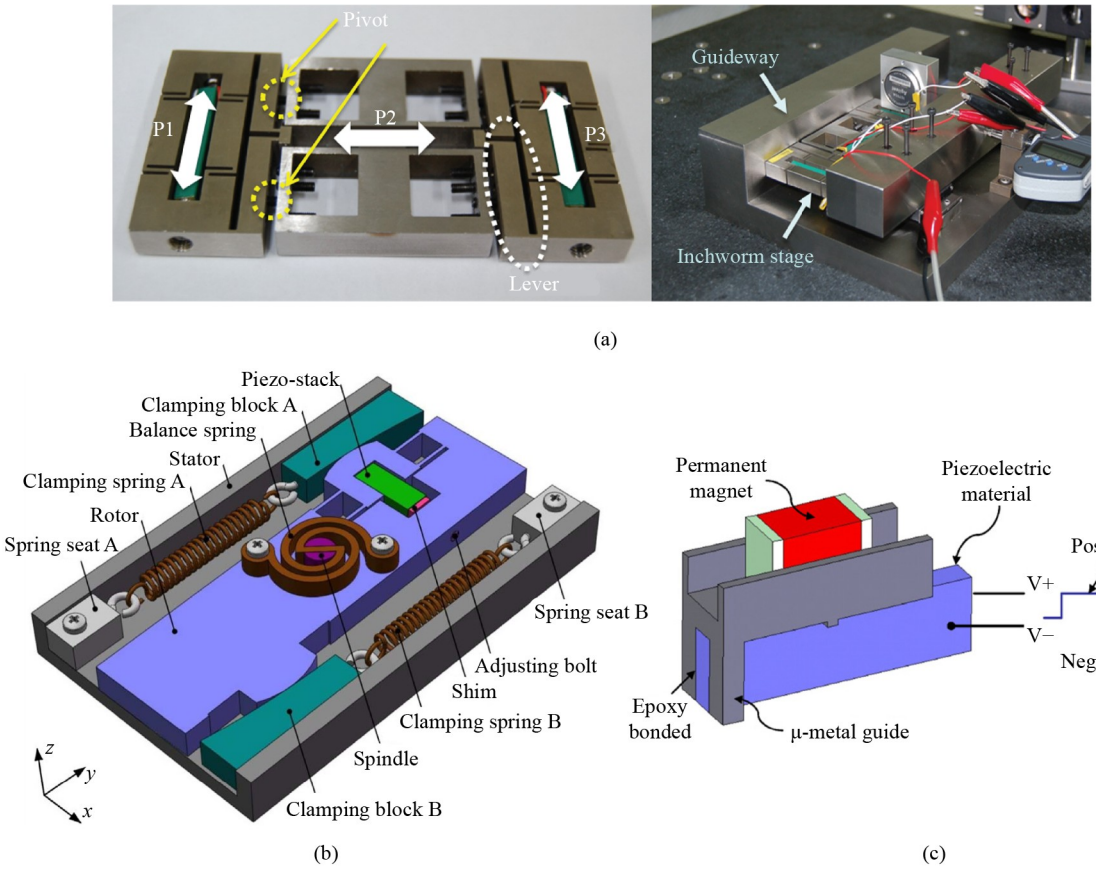

Fig. 22 Inchworm piezoelectric actuators combined with different structures: (a) inchworm actuator combine with flexible hinge [192], reproduced with permission from American Scientific Publishers; (b) improving performance with wedge blocks and springs [193], reproduced with permission from Elsevier; and (c) design of a permanent magnet structure is adopted [194], reproduced with permission from Elsevier.

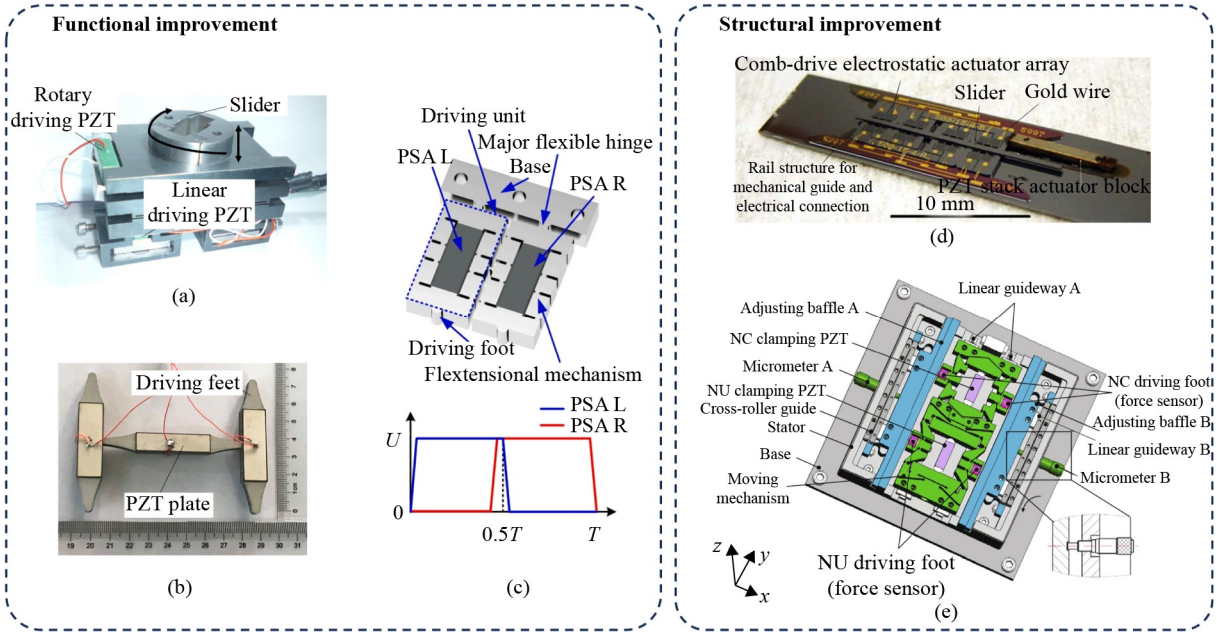

Fig. 23 Improvement of inchworm actuators: (a) prototype of the 2 degrees of freedom positioning [197], reproduced with permission from Elsevier; (b) prototype of high-speed inchworm actuator [195], reproduced under the terms of the CC BY license; (c) structure and exciting signals of inchworm actuator without "backlash" phenomenon [196], reproduced with permission from Elsevier; (d) miniaturized inchworm actuator [199], reproduced with permission from Institute of Physics Publishing; and (e) simplified design of inchworm actuator [198], reproduced with permission from Elsevier. NC: normally clamped, NU: normally unclamped, PSA: piezoelectric stack actuator, PZT: piezoelectric lead zirconate titanate.

output steps requires overcoming the "backlash" phenomenon. Theoretically, the inchworm piezoelectric actuator does not have this issue. However, the clamping or elongation mechanism may deform or rotate during the step process, leading to backward motions [200], which can be suppressed mainly through structural design [196, 201] (Fig. 23(c)). Multiple DOF can be realized through the combination of single DOF [202]. For example, Fuchiwaki et al. [203] designed a 3-DOF inchworm mobile mechanism, which achieved a resolution of less than 10 nm and a speed of 20 mm/s. However, the realization of multiple DOF may lead to the degradation of some attributes of the actuator, such as push force and speed [204], and thus is necessary to make trade-offs. Multiple degrees can also be transformed into various displacement output forms [197] (Fig. 23(a)), which will endow the inchworm actuator with more application scenarios.

The structure simplification aims to reduce the number of used PSAs [205], which may often use parasitic motion. Wang and Yan [198] proposed a bidirectional inchworm actuator driven by using only two PSAs (Fig. 23(e)), which achieves an output speed of 216.3 μm/s and an output force of 1.2 N. The miniaturization of the inchworm piezoelectric actuator has received attention [199] (Fig. 23(d)), and such a normally latched inchworm microactuator also helps to broaden the fields of application. One thing should be mentioned that the structure simplification also makes it more difficult to suppress the "backlash" phenomenon.

In summary, similar to the friction–inertial type, inchworm actuators enable unlimited stroke. The disadvantages of this kind of actuator include slow speed and high cost due to the complicated mechanical structure and control system. The discussed research works seem to conflict with each other because they have different targets. One should make a balance in design in accordance with requirements.

5 Comparison and selection

The categories of variants of piezoelectric actuators have been discussed in previous sections. Herein, Table 5 compares the advantages and disadvantages of different types of actuators and summarizes the characteristics more systematically. Figure 24 compares direct and indirect actuators in their most important performance parameters, including stroke and load capacity for direct actuators and load capacity and speed for indirect actuators. Typical demonstrations are selected as comparison cases to illustrate the most prominent characteristics of each type of actuator. The following conclusions are established for different types of piezoelectric actuators: In the direct type, the stack actuators have the best load capacity, and the structures with amplification mechanisms, such as flexible hinges, perform the best stroke. The stroke of the unimorph/bimorph actuators in Fig. 24(a) appears to be high

Table 5 Characteristics of different piezoelectric actuators

Actuation method	Type	Advantages	Disadvantages
Direct piezoelectric actuators	Membrane piezoelectric actuators	Simplest structure, excellent reliability, and repeatability	Short stroke and weak load capacity
	Multiple piezo stack actuators	Larger stroke, lower actuating voltage, rapid response time, higher stiffness and electromechanical coupling, and can withstand compression deformation	Cannot withstand tensile deformation
	Actuators with flexible hinges	Compact structure, smooth and repeatable motion, low inertial mass, low wear, and no "backlash" phenomenon	Weak output torque, poor overall stiffness, prominent stress concentration, and slow response speed
Indirect piezoelectric actuators	Standing wave actuators	Low cost (only a few driving sources needed), direct output displacement, and high efficiency	More severe wear
	Traveling wave actuators	Easy to implement bidirectional actuating	Lower efficiency, more complex structure, and difficult to miniaturize
	Friction–inertia actuators	Unlimited stroke, simple control system, and low cost	Slow speed, weak output torque, poor mass transport capacity, "backlash" phenomenon, accumulated errors, serious wear and short working life, and unable to achieve multiaxis motion
	Inchworm actuators	Unlimited stroke, better load capacity, repeatability, and reliability	Slightly worse accuracy, high cost, lower speed, complex control system, and mechanical structure

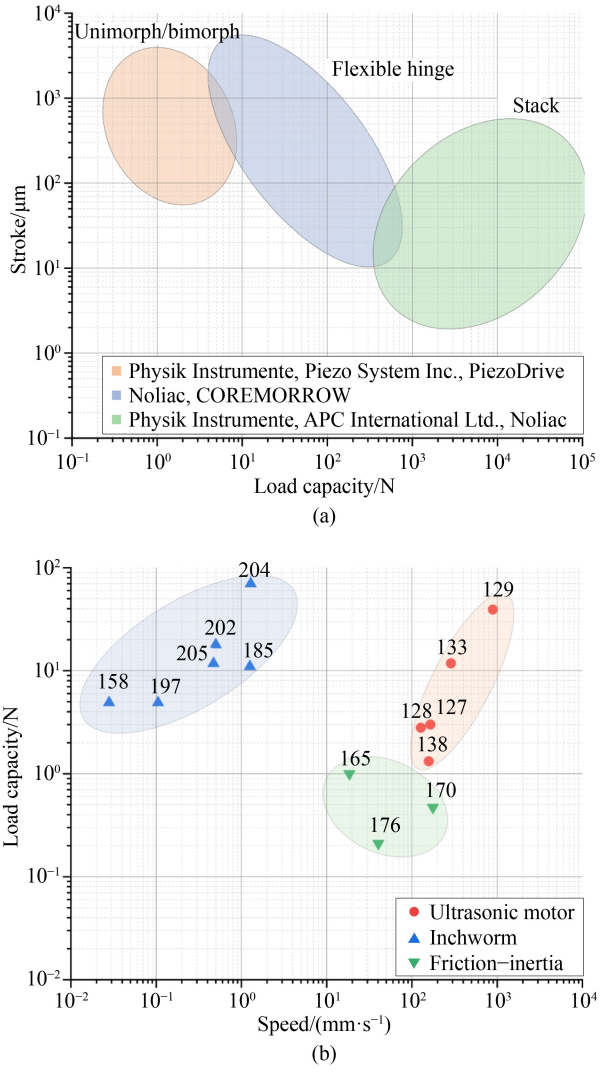

Fig. 24 Comparison of the performance of (a) direct and (b) indirect piezoelectric actuators (based on Refs. [206–211]).

because they usually denote the tip displacement or the displacement of the attached structure. The stroke of the unimorph/bimorph layer itself is only a fraction of the stack ones. In the indirect type, the ultrasonic motor has the fastest speed, and the inchworm piezoelectric actuators have the best load capacity. The friction–inertia piezoelectric actuators are relatively balanced due to the composition and driving principle.

From the point of view of industrial application, unimorph/bimorph piezoelectric actuators are more commonly used in the fields of microfluidics, micro-optics, precision instruments, etc., which have a high requirement of accuracy, reliability, and repeatability. Amplified piezoelectric actuators, including stack and flexible hinge-based actuators, are applicable in various mechanical structure designs, such as automation and robotics, in terms of their high load capacity, larger travel range, smooth displacement output, and design flexibility. Usually, amplified schemes are used in combination. Ultrasonic motors, as a new generation of motor actuators, have a fast response, high output efficiency, and immunity to electromagnetic interference; thus, they appeal to applications susceptible to electromagnetic interference, such as aerospace and medicine. Compared with ultrasonic motors, stepping actuators have a relatively slower output displacement speed but perform better structural flexibility, as shown in Fig. 24(b). They are widely used in various mechanical structure designs due to their low costs.

In conclusion, we believe that when choosing a feasible type of actuator for different application scenarios, multiple systemic factors should be considered, including but not limited to accuracy, speed, power consumption, structural complexity, control complexity, and cost. The above comparison and discussion can help guide the choices while considering the actual needs and final operational evaluations.

6 Conclusions and outlook

This work aims to provide a comprehensive and in-depth review of piezoelectric actuators. From the point of view

of principle, piezoelectric actuators are divided into direct and indirect types. Next, the fundamentals of piezoelectric actuators, including the piezoelectric constitutive equations and their respective forms under four different boundary conditions, are provided. Different kinds of piezoelectric materials are briefly reviewed, including single crystals, piezoelectric ceramics, and polymers. The working principle, pros and cons, and potential applications are discussed in detail for each mainstream actuator type. This work contributes to establishing the knowledge and understanding of different types of piezoelectric actuators. More importantly, the characteristics of all kinds of piezoelectric actuators mentioned are thoroughly compared, with the advantages and disadvantages identified. In engineering fields and development trends, valuable and in-depth content is expounded. Representative references for each specific type are also provided, along with their parameters listed in charts, which can help researchers or users choose the feasible type for their application scenarios.

Although great progress has been achieved in piezoelectric actuators because of researchers' unremitting efforts, they can still be improved, which may be the future research direction. As observed by the authors, some suggestions are listed below for reference:

The imperfection of the structural materials and phase mode-mistuning of excited waves often leads to impure waves driving ultrasonic motors (for example, partially standing waves appear in traveling waves). Therefore, future research should stimulate higher quality, purer, and more stable waves by studying various methods, such as the quality factor and mode match level of stator resonator, to improve ultrasonic motor efficiency and achieve stable operation.

The miniaturization (wafer-scale) of ultrasonic motors and the semiconductorization of manufacturing techniques reduce manufacturing costs, improve manufacturing precision, and enhance the capabilities of microelectromechanical system integration.

The research on stepping piezoelectric actuators will mainly focus on completely suppressing the "backlash" phenomenon in a broader range of situations and simplifying the structure of the actuator itself. Overcoming these two issues will help achieve smooth motion and further expand the application range of this type of actuator.

In addition to traditional PID or large-gain proportional derivative controllers, modern control strategies, such as adaptive control, robust control, and fuzzy control, combined with neural network models and machine learning methods (reinforcement learning, etc.), are used to improve the piezoelectric actuators' response to nonlinear behaviors, such as hysteresis and creep and its resistance to external interference, ultimately achieving improved trajectory tracking and high-precision positioning of the actuator.

More efficient and cost-effective optimization algorithms must be explored to optimize the structure of piezoelectric actuators. A new algorithm will help obtain higher quality local or global optimal solutions quickly under given conditions.

Nomenclature

Abbreviations

DOF	Degree of freedom
HAM	Hybrid-type amplification mechanism
IDA	Inertia/impact drive actuator
LAM	Lever-type amplification mechanism
PI	Physik Instrumente
PID	Proportional integral derivative
PMUT	Piezoelectric micromachined ultrasound transducer
PSA	Piezoelectric stack actuator
PVDF	Polyvinylidene fluoride
PZT	Piezoelectric lead zirconate titanate
RAINBOW	Reduced and internally biased oxide wafer
S–R	Scott–Russell
SSDA	Stick–slip drive actuator
SWM	Standing wave motor
TAM	Triangular-type amplification mechanism
TWM	Traveling wave motor
THUNDER	Thin layer unimorph driver

Variables

A	Amplitude of the standing wave
d_{15}, d_{31}, d_{33}	Piezoelectric coupling coefficients
D_i	Electrical displacement
h	Height of the single layer of piezoelectric material
k	Wavenumber whose value is equal to $2\pi/\lambda$
k_{33}	Electromechanical coupling factor
l	Length of the single layer of piezoelectric material
L	Output displacement
t	Time
T_c	Curie temperature
U	Voltage applied to the external electrodes
x	Coordinate of a certain position on the elastic body
ω	Angular frequency
λ	Wavelength of the standing wave

Acknowledgements This work was supported by the National Natural Science Foundation of China (Grant No. 62004166), Natural Science Foundation of Ningbo, China (Grant No. 202003N4062), Natural Science Foundation of Zhejiang Province, China (Grant No. LY23F040002), National Postdoctoral Program for Innovative Talents, China (Grant No. BX20200279), Natural Science Basic Research Program of Shaanxi

Province, China (Grant No. 2020JQ-199), and Fundamental Research Funds for the Central Universities, China (Grant No. 31020190QD027).

Conflict of Interest The authors declare that they have no conflict of interest.

References

1. Kumar D, Daudpoto J, Chowdhry B S. Challenges for practical applications of shape memory alloy actuators. Materials Research Express, 2020, 7(7): 073001
2. Gao C D, Zeng Z H, Peng S P, Shuai C J. Magnetostrictive alloys: promising materials for biomedical applications. Bioactive Materials, 2022, 8: 177–195
3. Ceyssens F, Sadeghpour S, Fujita H, Puers R. Actuators: accomplishments, opportunities and challenges. Sensors and Actuators A: Physical, 2019, 295: 604–611
4. Yuan Q, Kato B, Fan K Q, Wang Y. Phased array guided wave propagation in curved plates. Mechanical Systems and Signal Processing, 2023, 185: 109821
5. Uchino K. Advanced Piezoelectric Materials: Science and Technology. 2nd ed. Cambridge: Woodhead Publishing Ltd., 2017
6. Heywang W, Lubitz K, Wersing W. Piezoelectricity: Evolution and Future of a Technology. Heidelberg: Springer, 2008
7. Yang C, Youcef-Toumi K. Principle, implementation, and applications of charge control for piezo-actuated nanopositioners: a comprehensive review. Mechanical Systems and Signal Processing, 2022, 171: 108885
8. Wang S P, Rong W, Wang L F, Xie H, Sun L, Mills J K. A survey of piezoelectric actuators with long working stroke in recent years: classifications, principles, connections and distinctions. Mechanical Systems and Signal Processing, 2019, 123: 591–605
9. Mohith S, Upadhya A R, Navin K P, Kulkarni S M, Rao M. Recent trends in piezoelectric actuators for precision motion and their applications: a review. Smart Materials and Structures, 2021, 30(1): 013002
10. Zhang Z M, An Q, Li J M, Zhang W J. Piezoelectric friction–inertia actuator—a critical review and future perspective. The International Journal of Advanced Manufacturing Technology, 2012, 62(5–8): 669–685
11. Jeon J, Han C, Han Y M, Choi S B. A new type of a direct-drive valve system driven by a piezostack actuator and sliding spool. Smart Materials and Structures, 2014, 23(7): 075002
12. Xuan Z F, Jin T, Ha N S, Goo N S, Kim T H, Bae B W, Ko H S, Yoon K W. Performance of piezo-stacks for a piezoelectric hybrid actuator by experiments. Journal of Intelligent Material Systems and Structures, 2014, 25(18): 2212–2220
13. Chen F X, Zhang Q J, Gao Y Z, Dong W. A review on the flexure-based displacement amplification mechanisms. IEEE Access, 2020, 8: 205919–205937
14. Xu Q S, Li Y M. Analytical modeling, optimization and testing of a compound bridge-type compliant displacement amplifier. Mechanism and Machine Theory, 2011, 46(2): 183–200
15. Ding Y, Lai L J. Design and analysis of a displacement amplifier with high load capacity by combining bridge-type and Scott–Russell mechanisms. Review of Scientific Instruments, 2019, 90(6): 065102
16. Dong W, Chen F X, Gao F T, Yang M, Sun L N, Du Z J, Tang J, Zhang D. Development and analysis of a bridge-lever-type displacement amplifier based on hybrid flexure hinges. Precision Engineering, 2018, 54: 171–181
17. Spanner K, Koc B. Piezoelectric motors, an overview. Actuators, 2016, 5(1): 6
18. Hunstig M. Piezoelectric inertia motors—a critical review of history, concepts, design, applications, and perspectives. Actuators, 2017, 6(1): 7
19. Tian X Q, Liu Y X, Deng J, Wang L, Chen W S. A review on piezoelectric ultrasonic motors for the past decade: classification, operating principle, performance, and future work perspectives. Sensors and Actuators A: Physical, 2020, 306: 111971
20. Meitzler A H, Berlincourt D, Welsh F S, Tiersten H F, Coquin G A, Warner W A. IEEE Standard on Piezoelectricity. ANSI/IEEE, 1987
21. Voigt W. Crystal Physics Textbook. Leipzig and Berlin: B. G. Teubner, 1910
22. Cady W G. Piezoelectricity: An Introduction to the Theory and Applications of Electromechancial Phenomena in Crystals. New York: McGraw-Hill Book Company, Inc., 1946
23. Heising R A. Quartz Crystals for Electrical Circuits, Their Design and Manufacture. New York: D. Van Nostrand Company, Inc., 1946
24. Mason W. Hysteresis Losses in Solid Materials, Piezoelectric Crystals and Their Application in Ultrasonics. New York: Van Nostrand, 1950
25. Mindlin R D. On the equations of motion of piezoelectric crystals. In: Problems of Continuum Mechanics. Philadelphia: SIAM, 1989, 282–290
26. Tiersten H F, Mindlin R D. Forced vibrations of piezoelectric crystal plates. Quarterly of Applied Mathematics, 1962, 20: 107–119
27. Tiersten H F. Linear Piezoelectric Plate Vibrations: Elements of the Linear Theory of Piezoelectricity and the Vibrations Piezoelectric Plates. New York: Springer, 2013
28. Yang J S. An Introduction to the Theory of Piezoelectricity. Cham: Springer, 2005
29. Visintin A. Differential Models of Hysteresis. Heidelberg: Springer, 1994
30. Clayton G M, Tien S, Leang K K, Zou Q Z, Devasia S. A review of feedforward control approaches in nanopositioning for high-speed SPM. Journal of Dynamic Systems, Measurement, and

Control, 2009, 131(6): 061101
31. Sabarianand D V, Karthikeyan P, Muthuramalingam T. A review on control strategies for compensation of hysteresis and creep on piezoelectric actuators based micro systems. Mechanical Systems and Signal Processing, 2020, 140: 106634
32. Xu Q S. Adaptive integral terminal third-order finite-time sliding-mode strategy for robust nanopositioning control. IEEE Transactions on Industrial Electronics, 2021, 68(7): 6161–6170
33. Ling J, Feng Z, Zheng D D, Yang J, Yu H Y, Xiao X H. Robust adaptive motion tracking of piezoelectric actuated stages using online neural-network-based sliding mode control. Mechanical Systems and Signal Processing, 2021, 150: 107235
34. Qiu Z C, Chen G H, Zhang X M. Trajectory planning and vibration control of translation flexible hinged plate based on optimization and reinforcement learning algorithm. Mechanical Systems and Signal Processing, 2022, 179: 109362
35. Turner B L, Senevirathne S, Kilgour K, McArt D, Biggs M, Menegatti S, Daniele M A. Ultrasound-powered implants: a critical review of piezoelectric material selection and applications. Advanced Healthcare Materials, 2021, 10(17): 2100986
36. Vijaya M S. Piezoelectric Materials and Devices: Applications in Engineering and Medical Sciences. Boca Raton: CRC Press, 2012
37. Luan G D, Zhang J D, Wang R Q. Piezoelectric Transducers and Arrays. Revised ed. Beijing: Peking University Press, 2005 (in Chinese)
38. Lindon J C, Tranter G E, Koppenaal D W. Encyclopedia of Spectroscopy and Spectrometry. 3rd ed. Academic Press, 2017
39. Newnham R E, Cross L E. Ferroelectricity: the foundation of a field from form to function. MRS Bulletin, 2005, 30(11): 845–848
40. Zhang R, Jiang B, Cao W W, Amin A. Complete set of material constants of $0.93Pb(Zn_{1/3}Nb_{2/3})O_3$-$0.07PbTiO_3$ domain engineered single crystal. Journal of Materials Science Letters, 2002, 21(23): 1877–1879
41. Guo Y P, Luo H S, He T H, Pan X M, Yin Z W. Electric-field-induced strain and piezoelectric properties of a high curie temperature $Pb(In_{1/2}Nb_{1/2})O_3$-$PbTiO_3$ single crystal. Materials Research Bulletin, 2003, 38(5): 857–864
42. Park S E, Shrout T R. Ultrahigh strain and piezoelectric behavior in relaxor based ferroelectric single crystals. Journal of Applied Physics, 1997, 82(4): 1804–1811
43. Li F, Cabral M J, Xu B, Cheng Z X, Dickey E C, LeBeau J M, Wang J L, Luo J, Taylor S, Hackenberger W, Bellaiche L, Xu Z, Chen L Q, Shrout T R, Zhang S J. Giant piezoelectricity of Sm-doped $Pb(Mg_{1/3}Nb_{2/3})O_3$-$PbTiO_3$ single crystals. Science, 2019, 364(6437): 264–268
44. Nguyen C H. Interdigital-electrode thin-film piezoelectric microactuators. Dissertation for the Doctoral Degree. Borre: University of South-Eastern Norway, 2018
45. Zhang W, Xiong R G. Ferroelectric metal–organic frameworks. Chemical Reviews, 2012, 112(2): 1163–1195
46. Cross L E, Newnham R E. History of ferroelectrics. Ceramics and Civilization, 1987, 3: 289–305
47. Liu Y, Cai Y, Zhang Y, Tovstopyat A, Liu S, Sun C L. Materials, design, and characteristics of bulk acoustic wave resonator: a review. Micromachines, 2020, 11(7): 630
48. Berlincourt D A, Curran D R, Jaffe H. Piezoelectric and piezomagnetic materials and their function in transducers. Physical Acoustics: Principles and Methods, 1964: 169–270
49. Sawaguchi E. Ferroelectricity versus antiferroelectricity in the solid solutions of $PbZrO_3$ and $PbTiO_3$. Journal of the Physical Society of Japan, 1953, 8(5): 615–629
50. Jaffe B, Roth R S, Marzullo S. Piezoelectric properties of lead zirconate-lead titanate solid-solution ceramics. Journal of Applied Physics, 1954, 25(6): 809–810
51. Li J L, Qu W B, Daniels J, Wu H J, Liu L J, Wu J, Wang M W, Checchia S, Yang S, Lei H B, Lv R, Zhang Y, Wang D Y, Li X X, Ding X D, Sun J, Xu Z, Chang Y F, Zhang S J, Li F. Lead zirconate titanate ceramics with aligned crystallite grains. Science, 2023, 380(6640): 87–93
52. Mahapatra S D, Mohapatra P C, Aria A I, Christie G, Mishra Y K, Hofmann S, Thakur V K. Piezoelectric materials for energy harvesting and sensing applications: roadmap for future smart materials. Advancement of Science, 2021, 8(17): 2100864
53. Ramadan K S, Sameoto D, Evoy S. A review of piezoelectric polymers as functional materials for electromechanical transducers. Smart Materials and Structures, 2014, 23(3): 033001
54. Harrison J S, Ounaies Z. Polymers, piezoelectric. In: Schwartz M, ed. Encyclopedia of Smart Materials. John Wiley & Sons, 2002
55. Jones G D, Assink R A, Dargaville T R, Chaplya P M, Clough R L, Elliott J M, Martin J W, Mowery D M, Celina M C. Characterization, Performance and Optimization of PVDF as a Piezoelectric Film for Advanced Space Mirror Concepts. Technical Report SAND2005-6846, 2005
56. Chen Q X, Payne P A. Industrial applications of piezoelectric polymer transducers. Measurement Science & Technology, 1995, 6(3): 249
57. Kim J Y H, Cheng A, Tai Y C. Parylene-C as a piezoelectric material. In: Proceedings of 2011 IEEE the 24th International Conference on Micro Electro Mechanical Systems. Cancun: IEEE, 2011, 473–476
58. Park C, Ounaies Z, Wise K E, Harrison J S. *In situ* poling and imidization of amorphous piezoelectric polyimides. Polymer, 2004, 45(16): 5417–5425
59. Atkinson G M, Pearson R E, Ounaies Z, Park C, Harrison J S, Dogan S, Midkiff J A. Novel piezoelectric polyimide MEMS. In: Proceedings of TRANSDUCERS'03. The 12th International Conference on Solid-State Sensors, Actuators and Microsystems. Digest of Technical Papers (Cat. No. 03TH8664). Boston: IEEE, 2003, 782–785
60. Park K I, Lee M, Liu Y, Moon S, Hwang G T, Zhu G, Kim J E, Kim S O, Kim D K, Wang Z L, Lee K J. Flexible nanocomposite generator made of $BaTiO_3$ nanoparticles and graphitic carbons. Advanced Materials, 2012, 24(22): 2999–3004
61. Prashanthi K, Miriyala N, Gaikwad R D, Moussa W, Rao V R, Thundat T. Vibtrational energy harvesting using photo-patternable piezoelectric nanocomposite cantilevers. Nano Energy, 2013, 2(5): 923–932
62. Newnham R E, Skinner D P, Cross L E. Connectivity and piezoelectric−pyroelectric composites. Materials Research Bulletin, 1978, 13(5): 525–536
63. Sessler G M, West J E. Self-biased condenser microphone with high capacitance. The Journal of the Acoustical Society of America, 1962, 34(11): 1787–1788

64. Mohebbi A, Mighri F, Ajji A, Rodrigue D. Polymer ferroelectret based on polypropylene foam: piezoelectric properties prediction using dynamic mechanical analysis. Polymers for Advanced Technologies, 2017, 28(4): 476–483
65. Fang P, Wegener M, Wirges W, Gerhard R, Zirkel L. Cellular polyethylene-naphthalate ferroelectrets: foaming in supercritical carbon dioxide, structural and electrical preparation, and resulting piezoelectricity. Applied Physics Letters, 2007, 90(19): 192908
66. Nakayama M, Uenaka Y, Kataoka S, Oda Y, Yamamoto K, Tajitsu Y. Piezoelectricity of ferroelectret porous polyethylene thin film. Japanese Journal of Applied Physics, 2009, 48(9S1): 09KE05
67. Kang L H, Han J H. Prediction of actuation displacement and the force of a pre-stressed piezoelectric unimorph (PUMPS) considering nonlinear piezoelectric coefficient and elastic modulus. Smart Materials and Structures, 2010, 19(9): 094006
68. Zhu Y P, Liu W J, Jia K M, Liao W J, Xie H K. A piezoelectric unimorph actuator based tip-tilt-piston micromirror with high fill factor and small tilt and lateral shift. Sensors and Actuators A: Physical, 2011, 167(2): 495–501
69. Bakhtiari-Shahri M, Moeenfard H. Energy harvesting from unimorph piezoelectric circular plates under random acoustic and base acceleration excitations. Mechanical Systems and Signal Processing, 2019, 130: 502–523
70. Gao X Y, Yang J K, Wu J G, Xin X D, Li Z M, Yuan X T, Shen X Y, Dong S X. Piezoelectric actuators and motors: materials, designs, and applications. Advanced Materials Technologies, 2020, 5(1): 1900716
71. Yao L Q, Zhang J G, Lu L, Lai M O. Nonlinear static characteristics of piezoelectric bending actuators under strong applied electric field. Sensors and Actuators A: Physical, 2004, 115(1): 168–175
72. Wang Q M, Zhang Q M, Xu B M, Liu R B, Cross L E. Nonlinear piezoelectric behavior of ceramic bending mode actuators under strong electric fields. Journal of Applied Physics, 1999, 86(6): 3352–3360
73. Taleghani B K. Validation of high displacement piezoelectric actuator finite element models. In: Proceedings of proceedings of the Fifth European Conference on Smart Structures and Materials. Glasgow: SPIE, 2000, 17–45
74. Heo S, Wiguna T, Park H C, Goo N S. Effect of an artificial caudal fin on the performance of a biomimetic fish robot propelled by piezoelectric actuators. Journal of Bionics Engineering, 2007, 4(3): 151–158
75. Maaspuro M. Piezoelectric oscillating cantilever fan for thermal management of electronics and LEDs—a review. Microelectronics Reliability, 2016, 63: 342–353
76. Lee D O, Kang L H, Han J H. Active vibration isolation demonstration system using the piezoelectric unimorph with mechanically pre-stressed substrate. Journal of Intelligent Material Systems and Structures, 2011, 22(13): 1399–1409
77. Zhang S J, Zhao H F, Ma X F, Deng J, Liu Y X. A 3-DOF piezoelectric micromanipulator based on symmetric and antisymmetric bending of a cross-shaped beam. IEEE Transactions on Industrial Electronics, 2023, 70(8): 8264–8275
78. Zhou X X, Li K, Liu Y X, Sun J H, Li H Y, Chen W S, Deng J. Development of an antihydropressure miniature underwater robot with multilocomotion mode using piezoelectric pulsed-jet actuator. IEEE Transactions on Industrial Electronics, 2023, 70(5): 5044–5054
79. Haertling G H. Rainbow ceramics: a new type of ultra-high-displacement actuator. American Ceramic Society Bulletin, 1994, 73(1): 93–96
80. Hellbaum R F, Bryant R G, Fox R L, Antony N J Jr, Rohrbach W W, Simpson J O. Thin layer composite unimorph ferroelectric driver and sensor. US Patent 6734603 B2, 2004-5-11
81. Wise S A. Displacement properties of RAINBOW and THUNDER piezoelectric actuators. Sensors and Actuators A: Physical, 1998, 69(1): 33–38
82. Mossi K M, Bishop R P. Characterization of different types of high-performance THUNDER actuators. In: Proceedings of Smart Structures and Materials 1999: Smart Materials Technologies. Newport Beach: SPIE, 1999, 43–52
83. Gunda A, Özkayar G, Tichem M, Ghatkesar M K. Proportional microvalve using a unimorph piezoelectric microactuator. Micromachines, 2020, 11(2): 130
84. Roy K, Lee J E Y, Lee C K. Thin-film PMUTs: a review of over 40 years of research. Microsystems & Nanoengineering, 2023, 9(1): 95
85. Ci P H, Zhang L, Liu G X, Dong S X. Large electrical manipulation of permittivity in $BaTiO_3$ and $Pb(Zr,Ti)O_3$ bimorph heterostructure. Applied Physics Letters, 2014, 105(7): 072903
86. Uchino K. Ferroelectric Devices. 2nd ed. Boca Raton: CRC Press, 2018
87. Rios S A, Fleming A J. A new electrical configuration for improving the range of piezoelectric bimorph benders. Sensors and Actuators A: Physical, 2015, 224: 106–110
88. Karpelson M, Wei G Y, Wood R J. Driving high voltage piezoelectric actuators in microrobotic applications. Sensors and Actuators A: Physical, 2012, 176: 78–89
89. Ali A, Pasha R A, Elahi H, Sheeraz M A, Bibi S, Hassan Z U, Eugeni M, Gaudenzi P. Investigation of deformation in bimorph piezoelectric actuator: analytical, numerical and experimental approach. Integrated Ferroelectrics, 2019, 201(1): 94–109
90. Ghosh B, Jain R K, Majumder S, Roy S S, Mukhopadhyay S. Experimental characterizations of bimorph piezoelectric actuator for robotic assembly. Journal of Intelligent Material Systems and Structures, 2017, 28(15): 2095–2109
91. Jain R K, Majumder S, Ghosh B, Saha S. Design and manufacturing of mobile micro manipulation system with a compliant piezoelectric actuator based micro gripper. Journal of Manufacturing Systems, 2015, 35: 76–91
92. Hall A J, Riddick J C. Micro-electro-mechanical flapping wing technology for micro air vehicles. In: Proceedings of Bioinspiration, Biomimetics, and Bioreplication. San Diego: SPIE, 2012, 83390L
93. Hu J, Chen S, Wang L. A new insect-scale piezoelectric robot with asymmetric structure. IEEE Transactions on Industrial Electronics, 2023, 70(8): 8194–8202
94. Liu Y Z, Hao Z W, Yu J X, Zhou X R, Lee P S, Sun Y, Mu Z C, Zeng F L. A high-performance soft actuator based on a poly (vinylidene fluoride) piezoelectric bimorph. Smart Materials and

Structures, 2019, 28(5): 055011
95. Khan M U, Butt Z, Elahi H, Asghar W, Abbas Z, Shoaib M, Bashir M A. Deflection of coupled elasticity–electrostatic bimorph PVDF material: theoretical, FEM and experimental verification. Microsystem Technologies, 2019, 25(8): 3235–3242
96. Yuan Y H, Shyong Chow K, Du H J, Wang P H, Zhang M S, Yu S K, Liu B. A ZnO thin-film driven microcantilever for nanoscale actuation and sensing. International Journal of Smart and Nano Materials, 2013, 4(2): 128–141
97. Moradi-Dastjerdi R, Meguid S A, Rashahmadi S. Dynamic behavior of novel micro fuel pump using zinc oxide nanocomposite diaphragm. Sensors and Actuators A: Physical, 2019, 297: 111528
98. Ivan I A, Rakotondrabe M, Agnus J, Bourquin R, Chaillet N, Lutz P, Poncot J C, Duffait R, Bauer O. Comparative material study between PZT ceramic and newer crystalline PMN-PT and PZN-PT mateirals for composite bimorph actuators. Reviews on Advanced Materials Science, 2010, 24(15–16): 1–9
99. Kulikov A, Blagov A, Marchenkov N, Targonsky A, Eliovich Y, Pisarevsky Y, Kovalchuk M. $LiNbO_3$-based bimorph piezoactuator for fast X-ray experiments: static and quasistatic modes. Sensors and Actuators A: Physical, 2019, 291: 68–74
100. Ho S T, Jan S J. A piezoelectric motor for precision positioning applications. Precision Engineering, 2016, 43: 285–293
101. Zhang Y, Zhang W J, Hesselbach J, Kerle H. Development of a two-degree-of-freedom piezoelectric rotary-linear actuator with high driving force and unlimited linear movement. Review of Scientific Instruments, 2006, 77(3): 035112
102. Tolliver L, Xu T B, Jiang X N. Finite element analysis of the piezoelectric stacked-HYBATS transducer. Smart Materials and Structures, 2013, 22(3): 035015
103. Sahoo B, Panda P K. Fabrication of simple and ring-type piezo actuators and their characterization. Smart Materials Research, 2012, 2012: 821847
104. Gao X Y, Xin X D, Wu J G, Chu Z Q, Dong S X. A multilayered-cylindrical piezoelectric shear actuator operating in shear (d_{15}) mode. Applied Physics Letters, 2018, 112(15): 152902
105. Huang H H, Wang L F, Wu Y. Design and experimental research of a rotary micro-actuator based on a shearing piezoelectric stack. Micromachines, 2019, 10(2): 96
106. Jiang X N, Rehrig P W, Hackenberger W S, Smith E, Dong S X, Viehland D, Moore J Jr, Patrick B. Advanced piezoelectric single crystal based actuators. In: Proceedings of Smart Structures and Materials 2005: Active Materials: Behavior and Mechanics. San Diego: SPIE, 2005, 253–262
107. Liu R B, Wang Q M, Zhang Q M, Cross L E. Piezoelectric pseudo-shear mode actuator made by L-shape joint bonding. Journal of Materials Science Materials in Electronics, 1998, 9(6): 453–456
108. DeMiguel-Ramos M, Díaz-Durán B, Escolano J M, Barba M, Mirea T, Olivares J, Clement M, Iborra E. Gravimetric biosensor based on a 1.3 GHz AlN shear-mode solidly mounted resonator. Sensors and Actuators B: Chemical, 2017, 239: 1282–1288
109. Claeyssen F, Letty R L, Barillot F, Sosnicki O. Amplified piezoelectric actuators: static & dynamic applications. Ferroelectrics, 2007, 351(1): 3–14
110. Chen F X, Gao Y Z, Dong W, Du Z J. Design and control of a passive compliant piezo-actuated micro-gripper with hybrid flexure hinges. IEEE Transactions on Industrial Electronics, 2021, 68(11): 11168–11177
111. Dsouza R D, Navin K P, Theodoridis T, Sharma P. Design, fabrication and testing of a 2 DOF compliant flexural microgripper. Microsystem Technologies, 2018, 24(9): 3867–3883
112. Xu Q S. Design and smooth position/force switching control of a miniature gripper for automated microhandling. IEEE Transactions on Industrial Informatics, 2014, 10(2): 1023–1032
113. Sun X T, Chen W H, Tian Y L, Fatikow S, Zhou R, Zhang J B, Mikczinski M. A novel flexure-based microgripper with double amplification mechanisms for micro/nano manipulation. Review of Scientific Instruments, 2013, 84(8): 085002
114. Tian Y L, Shirinzadeh B, Zhang D W, Alici G. Development and dynamic modelling of a flexure-based Scott–Russell mechanism for nano-manipulation. Mechanical Systems and Signal Processing, 2009, 23(3): 957–978
115. Wu Q G, Yang D H, Li A H, Zhou G H, Yang B T. Design and test of a novel cost-effective piezo driven actuator with a two-stage flexure amplifier for chopping mirrors. In: Proceedings of Modern Technologies in Space- and Ground-based Telescopes and Instrumentation II. Amsterdam: SPIE, 2012, 84505G
116. Na T W, Choi J H, Jung J Y, Kim H G, Han J H, Park K C, Oh I K. Compact piezoelectric tripod manipulator based on a reverse bridge-type amplification mechanism. Smart Materials and Structures, 2016, 25(9): 095028
117. Chen F X, Du Z J, Yang M, Gao F T, Dong W, Zhang D. Design and analysis of a three-dimensional bridge-type mechanism based on the stiffness distribution. Precision Engineering, 2018, 51: 48–58
118. Juuti J, Kordás K, Lonnakko R, Moilanen V P, Leppävuori S. Mechanically amplified large displacement piezoelectric actuators. Sensors and Actuators A: Physical, 2005, 120(1): 225–231
119. Chen C M, Hsu Y C, Fung R F. System identification of a Scott–Russell amplifying mechanism with offset driven by a piezoelectric actuator. Applied Mathematical Modelling, 2012, 36(6): 2788–2802
120. Sashida T, Kenjo T. An Introduction to Ultrasonic Motors. Oxford: Clarendon Press, 1993
121. Zhao C S. Ultrasonic Motors: Technologies and Applications. Heidelberg: Springer, 2011
122. Izuhara S, Mashimo T. Design and characterization of a thin linear ultrasonic motor for miniature focus systems. Sensors and Actuators A: Physical, 2021, 329: 112797
123. Uchino K. Piezoelectric ultrasonic motors: overview. Smart Materials and Structures, 1998, 7(3): 273
124. Uchino K. Piezoelectric Actuators and Ultrasonic Motors. New York: Springer, 1996
125. Li S Y, Ou W C, Yang M, Guo C, Lu C Y, Hu J H. Temperature evaluation of traveling-wave ultrasonic motor considering interaction between temperature rise and motor parameters. Ultrasonics, 2015, 57: 159–166
126. Ryndzionek R, Sienkiewicz Ł. A review of recent advances in the single- and multi-degree-of-freedom ultrasonic piezoelectric

motors. Ultrasonics, 2021, 116: 106471
127. Ci P H, Liu G X, Chen Z J, Dong S X. A standing wave linear ultrasonic motor operating in face-diagonal-bending mode. Applied Physics Letters, 2013, 103(10): 102904
128. Wang L, Liu J K, Liu Y X, Tian X Q, Yan J P. A novel single-mode linear piezoelectric ultrasonic motor based on asymmetric structure. Ultrasonics, 2018, 89: 137–142
129. Liu Y X, Shi S J, Li C H, Chen W S, Liu J K. A novel standing wave linear piezoelectric actuator using the longitudinal-bending coupling mode. Sensors and Actuators A: Physical, 2016, 251: 119–125
130. He S P, Shi S J, Zhang Y H, Chen W S. Design and experimental research on a deep-sea resonant linear ultrasonic motor. IEEE Access, 2018, 6: 57249–57256
131. Jian Y, Yao Z Y, Silberschmidt V V. Linear ultrasonic motor for absolute gravimeter. Ultrasonics, 2017, 77: 88–94
132. Yeh C H, Su F C, Shan Y S, Dosaev M, Selyutskiy Y, Goryacheva I, Ju M S. Application of piezoelectric actuator to simplified haptic feedback system. Sensors and Actuators A: Physical, 2020, 303: 111820
133. Zhang Q, Chen W S, Liu Y X, Liu J K, Jiang Q. A frog-shaped linear piezoelectric actuator using first-order longitudinal vibration mode. IEEE Transactions on Industrial Electronics, 2017, 64(3): 2188–2195
134. Zhang B L, Yao Z Y, Liu Z, Li X N. A novel L-shaped linear ultrasonic motor operating in a single resonance mode. Review of Scientific Instruments, 2018, 89(1): 015006
135. Liu Y X, Chen W S, Liu J K, Shi S J. A cylindrical standing wave ultrasonic motor using bending vibration transducer. Ultrasonics, 2011, 51(5): 527–531
136. Liu J K, Xie T, Chen W S, Jia C H. A standing wave ultrasonic motor using longitudinal vibration transducers. Key Engineering Materials, 2011, 474–476: 661–665
137. Dabbagh V, Sarhan A A D, Akbari J, Mardi N A. Design and experimental evaluation of a precise and compact tubular ultrasonic motor driven by a single-phase source. Precision Engineering, 2017, 48: 172–180
138. Fan P Q, Shu X C, Yuan T, Li C D. A novel high thrust–weight ratio linear ultrasonic motor driven by single-phase signal. Review of Scientific Instruments, 2018, 89(8): 085001
139. Yeh C H, Su F C, Shan Y S, Dosaev M, Selyutskiy Y, Goryacheva I, Ju M S. Application of piezoelectric actuator to simplified haptic feedback system. Sensors and Actuators A: Physical, 2020, 303: 111820
140. Peng T J, Wu X Y, Liang X, Shi H Y, Luo F. Investigation of a rotary ultrasonic motor using a longitudinal vibrator and spiral fin rotor. Ultrasonics, 2015, 61: 157–161
141. Doshida Y, Tamura H, Tanaka S. High-power properties of crystal-oriented $(Sr,Ca)_2NaNb_5O_{15}$ piezoelectric ceramics and their application to ultrasonic motors. Japanese Journal of Applied Physics, 2019, 58(SG): SGGA07
142. Uchino K, Cagatay S, Koc B, Dong S, Bouchilloux P, Strauss M. Micro piezoelectric ultrasonic motors. Journal of Electroceramics, 2004, 13(1–3): 393–401
143. Zhou Y N, Chang J J, Liao X X, Feng Z H. Ring-shaped traveling wave ultrasonic motor for high-output power density with suspension stator. Ultrasonics, 2020, 102: 106040
144. Chen W S, Liu Y X, Yang X H, Liu J K. Ring-type traveling wave ultrasonic motor using a radial bending mode. IEEE Transactions on Ultrasonics, Ferroelectrics, and Frequency Control, 2014, 61(1): 197–202
145. Sun H Y, Yin H, Liu J, Zhang X L. Preload optimization method for traveling-wave rotary ultrasonic motor. Processes, 2021, 9(7): 1164
146. Jia B T, Wang L, Wang R F, Jin J M, Zhao Z H, Wu D W. A novel traveling wave piezoelectric actuated wheeled robot: design, theoretical analysis, and experimental investigation. Smart Materials and Structures, 2021, 30(3): 035016
147. Zhang J, Wang X Z. Design and experimental study of ultrasonic vibration feeding device with double symmetrical structure. IEEE Access, 2022, 10: 63481–63495
148. Uchino K. Piezoelectric motors for camera modules. In: Proceedings of International Conference on New Actuators. Bremen: International Center for Actuators and Transducers, 2008
149. Li Z, Wang Z, Guo P, Zhao L, Wang Q J. A ball-type multi-DOF ultrasonic motor with three embedded traveling wave stators. Sensors and Actuators A: Physical, 2020, 313: 112161
150. Ren W H, Yang M J, Chen L, Ma C C, Yang L. Mechanical optimization of a novel hollow traveling wave rotary ultrasonic motor. Journal of Intelligent Material Systems and Structures, 2020, 31(8): 1091–1100
151. Uchino K. Piezoelectric actuators 2006. Journal of Electroceramics, 2008, 20(3–4): 301–311
152. Pan Z Y, Wang L, Yang Y, Jin J M, Qiu J M. A novel bonded-type 3-degree-of-freedom ultrasonic motor: design, simulation, and experimental investigation. Smart Materials and Structures, 2023, 32(6): 065010
153. Leng J W, Jin L, Dong X X, Zhang H B, Liu C L, Xu Z K. A multi-degree-of-freedom clamping type traveling-wave ultrasonic motor. Ultrasonics, 2022, 119: 106621
154. Sun D, Tang Y J, Wang J, Wang X J. A novel fixable cylindrical ultrasonic motor. Advances in Mechanical Engineering, 2019, 11(3): 1–7
155. Liu J, Niu Z J, Zhu H, Zhao C S. Design and experiment of a large-aperture hollow traveling wave ultrasonic motor with low speed and high torque. Applied Sciences, 2019, 9(19): 3979
156. Niu R K, Liu J, Zhu H, Zhao C S. Design and evaluation of a novel light arc-shaped ultrasonic motor. AIP Advances, 2019, 9(6): 065009
157. Chen Y, Liu Q L, Zhou T Y. A traveling wave ultrasonic motor of high torque. Ultrasonics, 2006, 44: e581–e584
158. Cai J N, Chen F X, Sun L N, Dong W. Design of a linear walking stage based on two types of piezoelectric actuators. Sensors and Actuators A: Physical, 2021, 332: 112067
159. Pan C L, Zhang T, Dai T L, Han L L, Xia H J, Yu L D. Design and simulation of a 2-DOF parallel linear precision platform utilizing piezoelectric impact drive mechanism. In: Proceedings of the 10th International Symposium on Precision Engineering Measurements and Instrumentation. Kunming: SPIE, 2019, 110534B
160. Breguet J M, Clavel R. Stick and slip actuators: design, control,

performances and applications. In: Proceedings of the 1998 International Symposium on Micromechatronics and Human Science. Creation of New Industry (Cat. No. 98TH8388). Nagoya: IEEE, 1998, 89–95

161. Li J P, Huang H, Morita T. Stepping piezoelectric actuators with large working stroke for nano-positioning systems: a review. Sensors and Actuators A: Physical, 2019, 292: 39–51
162. Liu W H, Wang Y, Huang W Q, Ding Q J. A linear stepping piezoelectric motor using inertial impact driving. Applied Mechanics and Materials, 2012, 226–228: 693–696
163. Pan Q S, He L G, Pan C L, Xiao G J, Feng Z H. Resonant-type inertia linear motor based on the harmonic vibration synthesis of piezoelectric bending actuator. Sensors and Actuators A: Physical, 2014, 209: 169–174
164. Jiang N, Liu J B, Tao T, Han L. Motion characteristics of a rotary piezo impact drive mechanism. In: Proceedings of International Conference on Smart Materials and Nanotechnology in Engineering. Harbin: SPIE, 2007, 642324
165. Hua S M, Cheng G M, Zhang Z Y, Zeng P. Precise impact drive mechanism based on asymmetrically clamped piezoelectric actuator. Applied Mechanics and Materials, 2010, 37–38: 870–874
166. Wen J M, Ma J J, Zeng P, Cheng G M, Zhang Z H. A new inertial piezoelectric rotary actuator based on changing the normal pressure. Microsystem Technologies, 2013, 19(2): 277–283
167. Yamagata Y, Higuchi T, Saeki H, Ishimaru H. Ultrahigh vacuum precise positioning device utilizing rapid deformations of piezoelectric elements. Journal of Vacuum Science & Technology A, 1990, 8(6): 4098–4100
168. Higuchi T. Micro actuators using recoil of an ejected mass. IEEE Micro Robot and Teleoperators Workshop Proceedings, 1987, 16–21
169. Yokozawa H, Morita T. Wireguide driving actuator using resonant-type smooth impact drive mechanism. Sensors and Actuators A: Physical, 2015, 230: 40–44
170. Peng Y X, Liu L, Zhang Y K, Cao J, Cheng Y, Wang J. A smooth impact drive mechanism actuation method for flapping wing mechanism of bio-inspired micro air vehicles. Microsystem Technologies, 2018, 24(2): 935–941
171. Park M H, Chong H H, Lee B H, Jeong S S, Park T G. Study on the new type of piezoelectric actuator utilizing smooth impact drive mechanism. Ferroelectrics, 2016, 500: 218–228
172. Morita T, Yoshida R, Okamoto Y, Kurosawa M K, Higuchi T. A smooth impact rotation motor using a multi-layered torsional piezoelectric actuator. IEEE Transactions on Ultrasonics, Ferroelectrics, and Frequency Control, 1999, 46(6): 1439–1445
173. Yoshida R, Okamoto Y, Higuchi T, Hamamatsu A. Development of smooth impact drive mechanism (SIDM). Journal of the Japan Society for Precision Engineering, 1999, 65(1): 111–115
174. Deng J, Liu S H, Liu Y X, Wang L, Gao X, Li K. A 2-DOF needle insertion device using inertial piezoelectric actuator. IEEE Transactions on Industrial Electronics, 2022, 69(4): 3918–3927
175. Lee J, Kwon W S, Kim K S, Kim S. A novel smooth impact drive mechanism actuation method with dual-slider for a compact zoom lens system. Review of Scientific Instruments, 2011, 82(8): 085105
176. Mazeika D, Vasiljev P, Borodinas S, Bareikis R, Yang Y. Small size piezoelectric impact drive actuator with rectangular bimorphs. Sensors and Actuators A: Physical, 2018, 280: 76–84
177. Hunstig M, Hemsel T, Sextro W. Stick–slip and slip–slip operation of piezoelectric inertia drives—Part II: frequency-limited excitation. Sensors and Actuators A: Physical, 2013, 200: 79–89
178. Hunstig M, Hemsel T, Sextro W. Stick–slip and slip–slip operation of piezoelectric inertia drives. Part I: ideal excitation. Sensors and Actuators A: Physical, 2013, 200: 90–100
179. Cheng T H, Lu X H, Zhao H W, Chen D, He P, Wang L, Zhao X L. Performance improvement of smooth impact drive mechanism at low voltage utilizing ultrasonic friction reduction. Review of Scientific Instruments, 2016, 87(8): 085007
180. Li H Y, Li Y K, Cheng T H, Lu X H, Zhao H W, Gao H B. A symmetrical hybrid driving waveform for a linear piezoelectric stick–slip actuator. IEEE Access, 2017, 5: 16885–16894
181. Fan H Y, Tang J Y, Li T, Yang X F, Liu J H, Guo W X, Huang H. Active suppression of the backward motion in a parasitic motion principle (PMP) piezoelectric actuator. Smart Materials and Structures, 2019, 28(12): 125006
182. Deng J, Liu Y X, Li J, Zhang S J, Li K. Displacement linearity improving method of stepping piezoelectric platform based on leg wagging mechanism. IEEE Transactions on Industrial Electronics, 2022, 69(6): 6429–6432
183. Huang X, Hu Y L, Ma J J, Li J P, Lin H, Wen J M. An inertial piezoelectric rotary actuator based on active friction regulation using magnetic force. Smart Materials and Structures, 2021, 30(9): 095014
184. Koh J S, Cho K J. Omegabot: biomimetic inchworm robot using SMA coil actuator and smart composite microstructures (SCM). In: Proceedings of 2009 IEEE International Conference on Robotics and Biomimetics (ROBIO). Guilin: IEEE, 2009, 1154–1159
185. Ma L, Xiao J T, Zhou S S, Sun L N. A piezoelectric inchworm actuator of linear type using symmetrical lever amplification. Proceedings of the Institution of Mechanical Engineers, Part N: Journal of Nanoengineering and Nanosystems, 2015, 229(4): 172–179
186. Peng Y X, Peng Y L, Gu X Y, Wang J, Yu H Y. A review of long range piezoelectric motors using frequency leveraged method. Sensors and Actuators A: Physical, 2015, 235: 240–255
187. Stibitz G R. Incremental feed mechanisms. US Patent, 3138749, 1964-6-23
188. Douglas B A. Position control device. US Patent, 3377489A, 1968-4-9
189. Li J P, Wen J M, Hu Y L, Zhang Z H, He L D, Wan N. Principle, design and future of inchworm type piezoelectric actuators. In: Huang H, Li J P, eds. Piezoelectric Actuators. Rijeka: IntechOpen, 2021
190. Hsu S K, Albert B. Transducer. US Patent, 3292019, 1966-12-13
191. Fujimoto T. Linear motor driving device. US Patent, 4736131, 1988-4-5
192. Kim Y W, Choi S C, Park J W, Jung Y H, Lee D W. The characteristics of variable speed inchworm stage using lever mechanism by different materials. Journal of Nanoscience and

Nanotechnology, 2008, 8(11): 5696–5701
193. Wang S P, Rong W B, Wang L F, Pei Z C, Sun L N. A novel inchworm type piezoelectric rotary actuator with large output torque: design, analysis and experimental performance. Precision Engineering, 2018, 51: 545–551
194. Oh C H, Choi J H, Nam H J, Bu J U, Kim S H. Ultra-compact, zero-power magnetic latching piezoelectric inchworm motor with integrated position sensor. Sensors and Actuators A: Physical, 2010, 158(2): 306–312
195. Tian X Q, Quan Q Q, Wang L, Su Q. An inchworm type piezoelectric actuator working in resonant state. IEEE Access, 2018, 6: 18975–18983
196. Ma X F, Liu Y X, Deng J, Gao X, Cheng J F. A compact inchworm piezoelectric actuator with high speed: design, modeling, and experimental evaluation. Mechanical Systems and Signal Processing, 2023, 184: 109704
197. Li J P, Zhao H W, Qu X T, Qu H, Zhou X Q, Fan Z Q, Ma Z C, Fu H S. Development of a compact 2-DOF precision piezoelectric positioning platform based on inchworm principle. Sensors and Actuators A: Physical, 2015, 222: 87–95
198. Wang Y, Yan P. A novel bidirectional complementary-type inchworm actuator with parasitic motion based clamping. Mechanical Systems and Signal Processing, 2019, 134: 106360
199. Toda R, Yang E H. A normally latched, large-stroke, inchworm microactuator. Journal of Micromechanics and Microengineering, 2007, 17(8): 1715
200. Galante T, Frank J, Bernard J, Chen W, Lesieutre G A, Koopmann G H. Design, modeling, and performance of a high force piezoelectric inchworm motor. Journal of Intelligent Material Systems and Structures, 1999, 10(12): 962–972
201. Li J P, He L D, Cai J J, Hu Y L, Wen J M, Ma J J, Wan W. A walking type piezoelectric actuator based on the parasitic motion of obliquely assembled PZT stacks. Smart Materials and Structures, 2021, 30(8): 085030
202. Kang D, Kim J, Lee M G, Gweon D. Development of compact high precision two degree of freedom XY piezoelectric stepping positioner. Review of Scientific Instruments, 2008, 79(2): 026110
203. Fuchiwaki O, Arafuka K, Omura S. Development of 3-DOF inchworm mechanism for flexible, compact, low-inertia, and omnidirectional precise positioning: dynamical analysis and improvement of the maximum velocity within no slip of electromagnets. IEEE/ASME Transactions on Mechatronics, 2012, 17(4): 697–708
204. Tahmasebipour M, Sangchap M. A novel high performance integrated two-axis inchworm piezoelectric motor. Smart Materials and Structures, 2020, 29(1): 015034
205. Ma X F, Liu Y X, Deng J, Zhang S J, Liu J K. A walker-pusher inchworm actuator driven by two piezoelectric stacks. Mechanical Systems and Signal Processing, 2022, 169: 108636
206. PiezoDrive. Specifications of actuators. Available at PiezoDrive website, 2023-5-30
207. APC International Ltd. Specifications of actuators. Available at APC International Ltd. website, 2023-5-30
208. Physik Instrumente. Specifications of P-series actuators. Available at Physik Instrumente (PI) GmbH & Co. website, 2023-5-30
209. Noliac. Specifications of actuators. Avialable at CTS Corporation website, 2023-5-30
210. COREMORROW. Technical data of PSt series actuators. Available at Harbin Core Tomorrow Science and Technology Co., Ltd. website, 2023-5-30
211. Piezo Inc. Piezoelectric actuators & motors. Available at Piezo website, 2023-5-30